Computers & Graphics 37 (2013) 1012–1038

Contents lists available at ScienceDirect

Computers & Graphics

journal homepage: www.elsevier.com/locate/cag

Special Section on Advanced Displays

A survey on computational displays: Pushing the boundaries of optics, computation, and perception

Belen Masia [a,*], Gordon Wetzstein [b], Piotr Didyk [c], Diego Gutierrez [a]

[a] *Universidad de Zaragoza, Dpto. Informatica e Ing. de Sistemas. Maria de Luna, 1. 50018, Zaragoza, Spain*
[b] *MIT Media Lab, 75 Amherst St, Cambridge, MA 02139, USA*
[c] *MIT Computer Science and Artificial Intelligence Laboratory (CSAIL), 32 Vassar Street Cambridge, MA 02139 USA*

ARTICLE INFO

Article history:
Received 25 July 2013
Received in revised form
29 September 2013
Accepted 5 October 2013
Available online 17 October 2013

Keywords:
HDR display
Wide color gamut
High definition
Stereoscopic
Autostereoscopic
Automultiscopic

ABSTRACT

Display technology has undergone great progress over the last few years. From higher contrast to better temporal resolution or more accurate color reproduction, modern displays are capable of showing images which are much closer to reality. In addition to this trend, we have recently seen the resurrection of stereo technology, which in turn fostered further interest on automultiscopic displays. These advances share the common objective of improving the viewing experience by means of a better reconstruction of the plenoptic function along any of its dimensions. In addition, one usual strategy is to leverage known aspects of the human visual system (HVS) to provide apparent enhancements, beyond the physical limits of the display. In this survey, we analyze these advances, categorize them along the dimensions of the plenoptic function, and present the relevant aspects of human perception on which they rely.

1. Introduction

In 1692, French painter Gaspar Antoine de Bois-Clair introduced a novel technique that would allow him to paint the so-called *double portraits*. By dividing each portrait into a series of stripes carefully aligned behind vertical occluding bars, two different paintings could be seen, depending on the viewer's position with respect to the canvas. Fig. 1 shows the double portrait of King Frederik IV and Queen Louise of Mecklenburg-Gstow [1]. Later, Frederic Ives patented in 1903 what he called the *parallax stereogram*, based also on the idea of placing occluding barriers in front of an image to allow it to change depending on the viewer's position [2]. Five years later, Gabriel Lippmann proposed using a lenslet array instead, an approach he called *integral photography* [3].

Both parallax barriers and lenslet arrays shared a common objective: to provide different views of the same scene or, more technically, to increase the range and resolution of the angular dimension(s) of the *plenoptic function*. The plenoptic function [4] represents light observed from every position in every direction, i.e., a complete representation of the light in a scene. It is a multidimensional function that includes information about intensity, color (wavelength), time, position and viewing direction (angle). The previously mentioned techniques, for instance, allow to increase the angular resolution at the cost of reducing the spatial resolution (the same image area needs now to be shared between several views); an additional cost is reduced intensity, since parallax barriers block a large amount of light.

Over the past few years we have seen large advances in display technology. These have motivated surveying papers on related topics such as real-time image correction techniques for projector–camera systems [5], parallax capabilities of 3D displays [6,7], or specialized courses focused on emerging compressive displays in top conferences [8,9], to name just a few.

In this survey, we provide a holistic view of the field, mainly from a computer graphics perspective, and categorize existing works according to which particular dimension(s) of the plenoptic function is enhanced. For instance, high dynamic range displays improve intensity (luminance) contrast, while automultiscopic displays expand angular resolution. We further note that the recent progress in the field has been spurred by the *joint design* of hardware and display optics with computational algorithms and perceptual considerations. Thus, we identify perceptual aspects of the human visual system (HVS) that are being used by these technologies to yield an *apparent* enhancement, beyond the physical possibilities of the display. Examples of these include wobbling displays, providing higher spatial resolution by retinal integration of lower resolution images, or the apparent increased intensity of some pixels caused by the glare illusion.

Therefore, we provide a novel view of the recent advances in the field taking the plenoptic function as a supporting structure

* Corresponding author. Tel.: +34 976762353.
E-mail address: bmasia@unizar.es (B. Masia).

0097-8493/$ - see front matter © 2013 Elsevier Ltd. All rights reserved.
http://dx.doi.org/10.1016/j.cag.2013.10.003

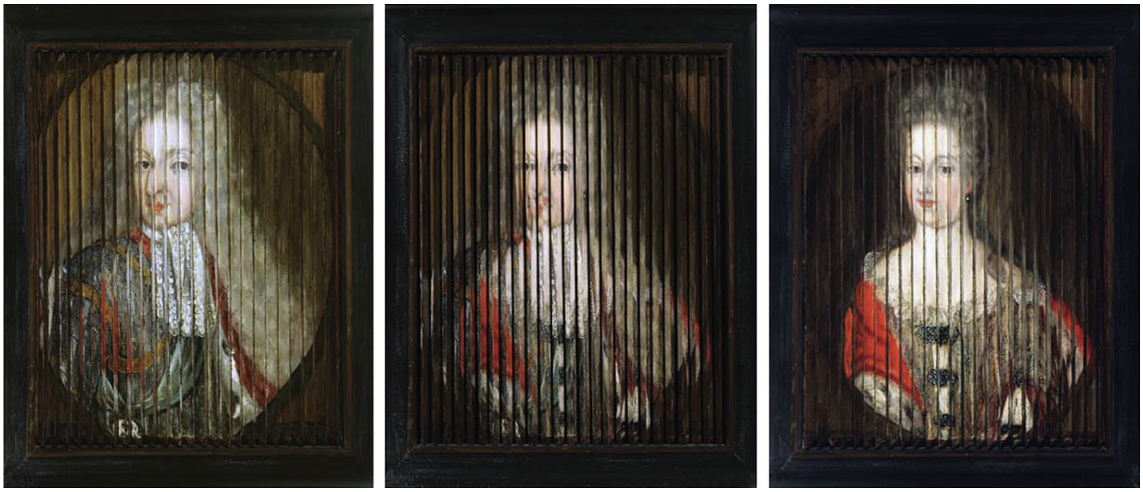

Fig. 1. Double portrait by Gaspar Antoine de Bois-Clair, as viewed from the left, center and from the right (images courtesy of Robert Simon [1]).

	Contrast and Luminance Range	Color Gamut	Spatial Resolution	Temporal Resolution	Angular Resolution I - Stereo	Angular Resolution II - Automultiscopic
Perceptual Considerations	Dynamic range of the eye (photopic-mesopic-scotopic vision), dynamic adaptation, CSF, Craik-O'Brien-Cornsweet illusion, visual masking	Dual-process theory, trichromatic & color-opponent stages, chromatic adaptation, standardized observers	Photoreceptor density, foveal and peri-foveal vision, SPEM	Temporal integration, Bloch's law, CFF, hold-type blur, SPEM	Panum's fusional area, zone of comfort, acc.-vergence conflict, DSF, Craik-O'Brien-Cornsweet illusion for depth, disparity models	Disparity models, motion parallax, accommodation, cue integration
Display Architectures	Two-layer optical modulation	Increasing the purity of primaries	Optical superposition	Backlight flashing	Spatial multiplexing (anaglyph, polarization)	Volumetric displays
	Local dimming	Multi-primary displays	Temporal superposition		Temporal multiplexing (shutter glasses)	Light field displays
	Multi-projector systems	Projection systems	Optical Pixel Sharing		Backward-compatible stereo	Compressive light field displays
					Autostereoscopic	Light field displays supporting accommodation
Content Generation	HDR image/video acquisition	Color Appearance Models	Super-resolution	Black data insertion	Camera parameters adjustment	Efficient image synthesis
	Apparent brightness enhancement	Gamut mapping	Sub-pixel rendering	Frame interpolation techniques	Disparity remapping	Light field retargeting
	Tone mapping	Radiometric calibration	Temporal integration	Motion compensated inverse filtering	Microstereopsis and Backward-compatible stereo	Disparity remapping
	Reverse tone mapping			Warping techniques		Multiview from stereo
				Leveraging information from the rendering pipeline		
				Mesh-based temporal upsampling		

Fig. 2. Overview of architectures and techniques, according to the structure followed in this survey. Columns in the table correspond to dimensions of the plenoptic function, and to the sections of this paper. For each section, we first discuss relevant perceptual aspects (related keywords are shown in the first row of this table), then describe display architectures (middle row), and finally present software solutions and content generation approaches aimed at improving the corresponding dimension of the plenoptic function (third row).

(see Fig. 2) and putting an emphasis on human visual perception. For each section, each focusing on a dimension of the plenoptic function, we first present perceptual foundations related to that dimension, and then describe display technologies, and software solutions for the generation of content in which the specific dimension being discussed is enhanced. Specifically, we first address expansion on dynamic range in Section 2, followed by color gamut (Section 3), increased spatial resolution (Section 4), increased temporal resolution (Section 5) and finally increased angular resolution, for both stereo (Section 6) and automultiscopic displays (Section 7).

For topics where there is a large body of existing literature, beyond what can be reasonably covered by this survey, we highlight some of the main techniques and suggest alternative publications for further reading (this is the case of, e.g., tone mapping or superresolution techniques). For other related aspects not covered here, such as detailed descriptions of hardware, electronics or the underlying physics of the hardware, we refer the interested reader to other excellent sources [10,11]. Finally, although projection-based display systems are included in this survey whenever they focus on enhancing the aspects of the plenoptic function, there are a number of works which fall out of the scope of this survey. These include works dealing with geometric calibration (briefly discussed in Section 3.3), or extended depth-of-field projection [12,13]. We refer the interested reader to existing books and tutorials focused on projection systems [14,5,15].

2. Improving contrast and luminance range

The *dynamic range* of a display refers to the ratio between the maximum and minimum luminance that the display is capable of emitting [16]. The advantages and improved quality of High Dynamic Range (HDR) images are by now well established. By not limiting the values of the red, green and blue channels to the range [0..255], physically accurate photometric values can be stored instead. This yields much richer depictions of the scenes,

Fig. 3. Low dynamic range depictions of a high dynamic range scene, showing large saturated (left) or dark areas (right).

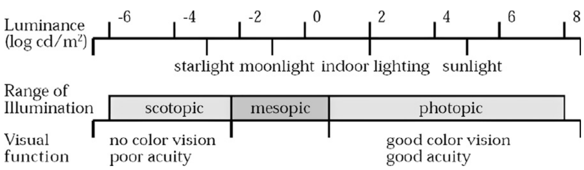

Fig. 4. Scotopic, mesopic and photopic vision, corresponding to different luminance levels (image from [23], copyright T. Aydin 2010).

including more detail in dark areas and avoiding saturated pixels (Fig. 3).

Many applications can benefit from HDR data, including image-based lighting [17], image editing [18] or medical imaging [19]. The field has been extensively investigated, especially in the last decade, and several excellent books exist offering detailed explanations on related aspects, including image formats and encodings, capture methods, or quality metrics [16,20–22].

2.1. Perceptual considerations

There are two types of photoreceptors in the eye: cones and rods. Each of the three cone types is sensitive in a wavelength range, the sensitivity of each type peaking at a different wavelength, roughly belonging to red, green and blue; combined, they allow us to see color. They are most sensitive to *photopic* (day light) luminance conditions, usually above 1 cd/m^2, while rods (of which only one type exists) are most sensitive to *scotopic* (night light) conditions, approximately below 10^{-3} cd/m^2. The bridging range where both cones and rods play an active role at the same time is called the *mesopic* range (see Fig. 4).

On the other hand, luminance values in natural scenes (from moonless night sky to direct sunlight from a clear sky) may span about 12–14 orders of magnitude, although simultaneous luminance values usually fall within a more restricted range of about 4–6 orders of magnitude (for a more exhaustive discussion on luminance ranges in natural scenes the reader may refer to [24]). The HVS can perceive only around four orders of magnitude simultaneously, but it uses a process known as dynamic *adaptation*, effectively shifting its sensitive range to the current illumination conditions [16,25,26].

Despite this ability to adapt across a wide dynamic range, our ability to discern local scene contrast boundaries is reduced by veiling caused by light scattering inside the eye (an effect known as veiling glare, or disability glare). Many other luminance-related factors affect our visibility, including the intensity of the background (Weber's law) and the spatial frequency of the stimuli, whose dependency is modeled by the contrast sensitivity function (CSF, see Fig. 5, right); the bleaching of photoreceptors when exposed to high levels of luminance, which translates into a loss of spectral sensitivity [27]; the Craik–O'Brien–Cornsweet illusion, by which adjacent regions of equal luminance are perceived differently depending on the characteristics of their shared edges [28]; or the effect known as visual masking, where contrast sensitivity loss is induced due to the presence of signal in nearby regions [23]. Researchers have also investigated perceptual aspects of increased dynamic range, including analyzing the subjective preferences of users, to improve HDR display technology [29–31].

2.2. Display architectures

Traditional CRT displays typically show up to two orders of magnitude of dynamic range: analog display signals are typically 8-bit because, even though a CRT display could reproduce higher bit-depths, it would be including values at levels too low for humans to perceive [16]. LCD displays, although brighter, do not significantly improve that range. HDR displays enhance the contrast and luminance range of the displayed images, thus providing a richer visual experience. A passive HDR stereoscopic viewer overlaying two transparencies was presented by Ledda et al. [32]. Seetzen et al. [33,34] presented the first two active prototypes, which set the basis for later models that can be now found in the market (Fig. 5, left). The two prototypes shared the key idea illustrated in Fig. 5, center—of optically modulating a high spatial resolution (but low dynamic range) image with an LCD panel showing a grayscale, low spatial resolution (but high intensity) version of the same image. This provides a theoretical contrast equal to the multiplication of both dynamic ranges. Alternatively, two parallel-aligned LCD panels of equal resolution can be used [35]. A detailed description of the first prototypes and the concept of *dual modulation* of light can be found in Seetzen's Ph.D. Thesis [36].

Commercially available displays with increased contrast are mostly based on *local dimming*. This name refers to the particular case of dual modulation in which one of the modulators has a significantly lower resolution than the other [16]. This arises from knowledge of visual perception, and in particular of the effect known as veiling glare. Due to veiling glare, the contrast that can be perceived at a local level is much lower than at a global level, meaning that there is no need to have very large local contrast, and thus a lower resolution panel can be used for one of the modulators. The drawback is potentially perceivable halos, whose visibility depends on the particular arrangement of the LED array.

Projector-based systems exist, also based on the principle of double modulation. Majumder and Welch showed how by overlapping multiple projectors, the intensity range (difference between highest and lowest intensity levels; note that it is different from contrast, which is defined as the ratio) could be increased [38]. The first contrast expansion technique was proposed by Pavlovych and Stuerzlinger [39], where a small projected image is first formed by a set of lenses, which is subsequently modulated by an LCD panel. A second set of lenses enlarges the final image. Other similar approaches exist, making use of LCD or LCoS panels to modulate the illumination [40,41]. Multi-projector tiled displays present another problem in addition to limited dynamic range: brightness and color discontinuities at the overlapping projected areas [42]. Majumder et al. [43] rely on the

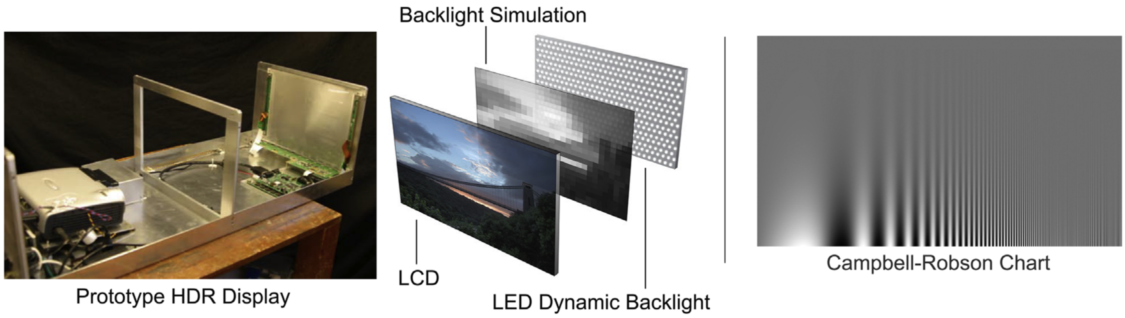

Fig. 5. Left: The first HDR prototype display, employing dual modulation (image from [34], copyright ACM 2004). Center: scheme illustrating the functioning of dual modulation, please refer to the text for details (image source: LCDTV Buying Guide). Right: the contrast sensitivity function, represented by a Campbell–Robson chart [37]; the abscissa corresponds to increasing spatial frequencies, the ordinate to decreasing amplitude of the contrast. The chart shows that the sensitivity of the HVS to contrast depends on the spatial frequency of the signal, and follows an inverted U-shape.

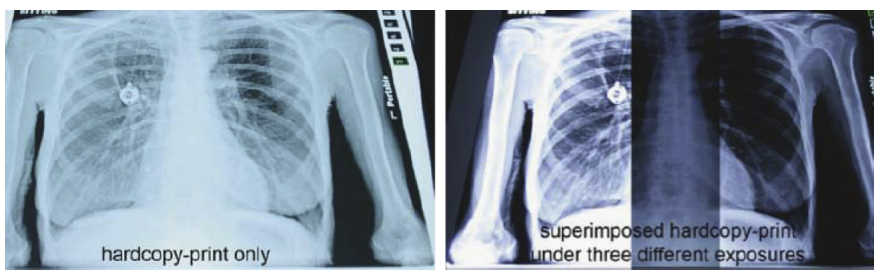

Fig. 6. Superimposing dynamic range for medical applications. Left: a single hardcopy print. Right: expanded dynamic range by superimposing three different prints with different exposures [19] (image copyright ACM 2008).

contrast sensitivity function to achieve a seamless integration with enhanced overall brightness. Recently, secondary modulation of projected light has also been used to boost contrast of paper images and printed photographs [19] (see Fig. 6).

2.3. HDR content generation and processing

Contrast and accurate depiction of the dynamic range of real world scenes have been a key issue in photography for over a century (see for instance the work of Ansel Adams [44]). The seminal works by Mann and Picard [45], and by Debevec and Malik [46], brought HDR imaging to the digital realm, allowing to capture HDR data by adapting the multi-bracketing photographic technique. More sophisticated acquisition techniques have continued to appear ever since (see [47] for a compilation), helping for instance to reduce ghosting artifacts in dynamic scenes [48–50] (see [51] for a recent review on deghosting techniques), using computational photography approaches [52,53], mobile devices [54,55] or directly capturing HDR video [56,22,57,58].

Regarding the visualization of such HDR content, we distinguish three main categories: tone-mapping, by which high dynamic range is scaled down to fit the capabilities of the display; reverse tone mapping, by which low dynamic range is expanded for correct visualization on more modern higher dynamic range displays; and apparent brightness enhancement techniques, which leverage how our brains interpret some specific luminance cues and translate them into the perception of brightness (but the actual dynamic range remains unchanged).

Tone mapping: Over the past few years, many user studies have been performed to understand which tone mapping strategies produce the best possible visual experience [59,29,30,60]. The field has been extremely active over the past two decades, with a proliferation of many algorithms which can be broadly characterized as global or local operators. While a complete survey of all existing tone mapping operators is out of the scope of the work, the interested reader can refer to other sources of information, where many of these algorithms are discussed, categorized and compared [61,16,20,62].

Global operators apply the same mapping function to all the pixels in the image, and were first introduced to computer graphics by Tumblin and Rushmeier [64]. They can be very simple, although they may fail to reproduce fine details in areas where the local contrast cannot be maintained [65,66]. To provide results that better simulate how real-world scenes are perceived, usually some perceptual strategies are adopted, based on different aspects of the HVS [67–70]. Usually these perceptually motivated works rely on techniques like multi-scale representations, transducer functions, color appearance models or retinex-based algorithms [71].

Local operators, on the other hand, tone-map each pixel taking into account information from the surrounding pixels, and thus usually allow for better preservation of local contrast [72]. The main drawback is that the local nature of the algorithms may give rise to unpleasant halos around some edges [16]. Again, perceptual considerations can be introduced in their design to reduce visible artifacts [73,74]. Other strategies include adapting well known analog tone reproduction techniques from photography [63] (Fig. 7), while others take into account the temporal domain, being especially engineered for videos [75].

Other operators work from a different perspective, for instance by working in the gradient domain [76] or in the frequency domain [77]. The exposure fusion technique [78] circumvents the need to obtain an HDR image first and *then* apply a tone mapping operator. Instead, the final tone-mapped image is directly assembled from the original multi-bracketed image sequence, based on simple, pixel-wise quality measures. Last, the work by Mantiuk et al. [79] derives a tone mapping operator that takes explicitly into account the different displays and viewing conditions the images can be viewed under.

Reverse tone mapping: Somewhat less studied is the problem of *reverse* tone mapping, where the goal is to take LDR content and expand its contrast to recreate an HDR viewing experience. This is

Fig. 7. Tone mapping allows for a better visualization of HDR images on displays with a limited dynamic range. Left, naive visualization with a simple linear scaling; right, the result of Reinhard's photographic tone reproduction technique [63] (image copyright ACM 2002). Radiance map courtesy of Cornell Program of Computer Graphics.

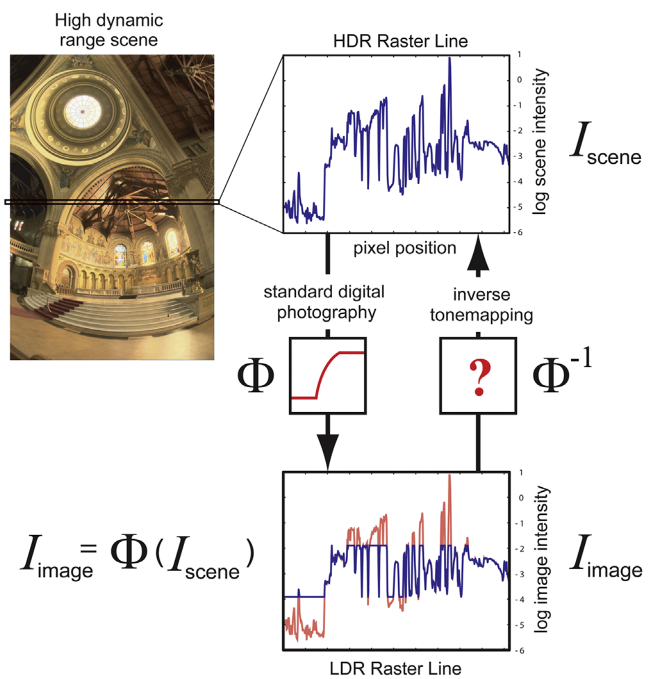

Fig. 8. The reverse tone mapping problem. Standard imaging loses dynamic range by transforming the raw scene intensities I_{scene} through some unknown function Φ, which clips and distorts the original scene values to create the I_{image} (clipped values shown in red). The goal of reverse tone mapping is to invert Φ to reconstruct the original luminance. Adapted from [81] (copyright ACM 2009). (For interpretation of the references to color in this figure caption, the reader is referred to the web version of this paper.)

gaining importance as more and more HDR displays reach the market, given the large amount of LDR legacy content. Reverse tone mapping involves dealing with clipped data, which makes it a slightly different problem from tone mapping (see Fig. 8). As before, a number of studies have been conducted to understand what the best strategy for dynamic range expansion may be [31,80–83].

The first methods were presented by Daly and Feng, and included bit-depth extension techniques [84] followed by techniques to solve subsequent problems such as contour artifacts [85]. More works have appeared over the years, usually following the approach of identifying the bright areas in the input image and expanding those the most, leaving the rest moderately (if at all) expanded to prevent noise amplification [86–90]. Other methods require direct user input [91–93]. Banterle and colleagues proposed one of the first extensions for video [94], while Masia et al. analyzed the problem across varying exposure conditions [81,95]. In their work, the authors additionally found that the perceived quality of the expanded images depends more on the absence of disturbing spatial artifacts than on the exact contrasts in the image. A more exhaustive presentation on the topic of reverse tone mapping can be found in the recent book by Banterle et al. [20].

Apparent brightness enhancement: A strategy to increase the *apparent* dynamic range of the displayed images is to directly exploit some of the mechanisms of the HVS, and how our brains interpret some luminance cues, and translate them into the perception of brightness. For instance, we have mentioned how some tone mapping operators introduce unwanted halos, that are perceived as artifacts. However, halos have been used for centuries by painters, to create steeper luminance gradients at the edges of objects and increase local image contrast. This technique is known as *counter-shading*, and it resembles the *unsharp masking* operator, which increases local contrast by adding a high-pass-filtered version of the image [96–99]. The potential benefits and drawbacks of this technique have also been recently investigated in this context [100].

Another example is the *bleaching effect*, which was first utilized by Gutierrez and colleagues to both increase apparent brightness of light sources and simulate the associated perceived change of color [101,102]. The temporal domain was subsequently added, allowing for the simulation of time-varying afterimages [103] (see Fig. 9). Synthetic glare has also been added around bright light sources in the images, to simulate scattering (both in the atmosphere and in the eye) and thus enhance brightness [104,105]. Last, binocular fusion has been used by showing two different low dynamic range depictions of the same HDR input image on a binocular display. The fused image presents more visual richness and detail than any of the single LDR versions [106] (Fig. 10).

3. Improving color gamut

In 1916 the company Technicolor was granted a patent for "a device for simultaneous projection of two or more images" [107] which would allow the projection of motion pictures in color. Although not the only color film system, it would be the system primarily used by Hollywood companies for their movies in the first half of the 20th century. Color television came later, starting in 1950 in the United States (although NTSC was not introduced until 1953), and not reaching Europe until 1967 (PAL/SECAM systems). Several standards are in use today, among which YCbCr is the ITU-R recommendation for HDTV (high definition television, with a standard resolution of 720p or 1080p). Until today, the quest to reproduce the whole color range that our visual system can perceive continues.

3.1. Perceptual considerations

The *dual-process theory* is the commonly accepted theory that describes the processing of color by the HVS [37]. The theory states that color processing is performed in two sequential stages: a

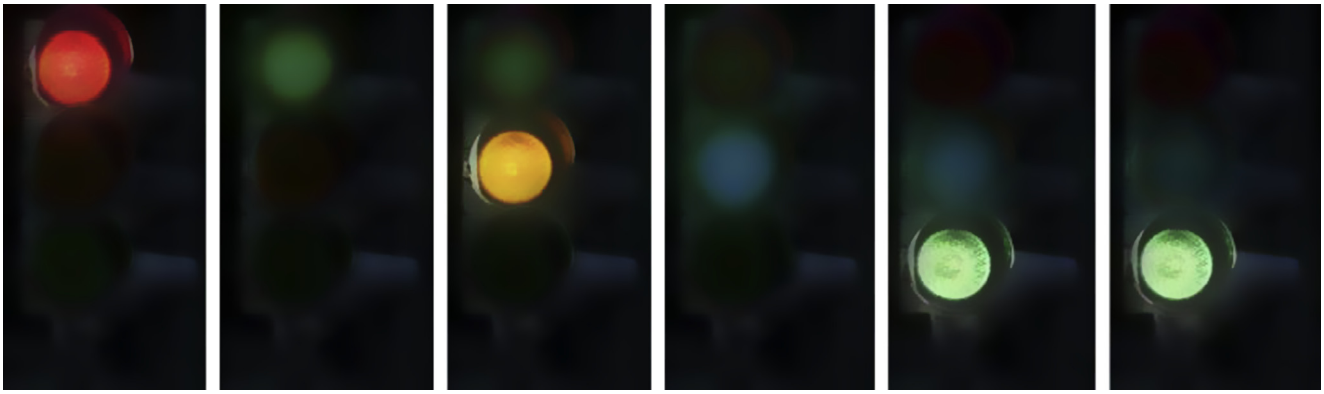

Fig. 9. Afterimage simulation of a traffic light, showing variations over time of color, degree of blur and shape [103] (image copyright Wiley 2012). (For interpretation of the references to color in this figure caption, the reader is referred to the web version of this paper.)

Fig. 10. Binocular tone mapping. When the two images are presented simultaneously to both eyes (one to each eye), the fused image presents more detail than any of the two individual, low dynamic range depictions [106] (image copyright ACM 2012).

trichromatic stage and an opponent-process stage [108]. The trichromatic stage is based on the theory that any perceivable color can be generated with a combination of three colors, which correspond to the three types of color-perceiving photoreceptors of our visual system (see Section 2.1). In the opponent-process stage the three channels of the previous stage are re-encoded into three new channels: a red-green channel, a yellow-blue channel, and a non-opponent channel for achromatic responses (from black to white). These theories, originally developed by psychophysics, are confirmed by neurophysiological results.

The theories which have been mentioned describe the behavior of the HVS for isolated patches of color, and do not take into account the influence of surrounding factors, such as environment lighting. *Chromatic adaptation* (or color constancy), for instance, is the mechanism by which our visual system adapts to the dominant colors of illumination. There are many other mechanisms and effects that play a role in our perception of color, such as simultaneous contrast, the brightness of colors, image size or the luminance level of the surroundings, and many experiments have been carried out to try to quantify them [109–113]. Recently, edge smoothness was also found to have a measurable impact on our perception of color [114,115]. Further, color perception has a large psychological component, making it a challenging task to measure, describe or reproduce color. So-called "standardized" observers exist [37,116], based on measurements of a set of observers, and are used as a reference for display design, manufacturing or calibration.

3.2. Display architectures

Increasing the color gamut of displays is typically achieved by using more saturated primaries, or by using a larger number of primaries. The former essentially "pushes further" the corners of the triangle defining the color gamut in a three-primary system; an alternative technique consists of using negative values for the RGB color signals [117]. Emitting elements with a broad spectral distribution, as is the case of phosphors in CRTs, severely limit the achievable gamut. Research has been carried out to improve the color gamut of these types of displays [118], but for the last two decades liquid crystal displays have been the most common display technology due to their advantages over CRTs [119,120]. Progressively, the traditional CCFL (cold cathode fluorescent lamp) backlights used in these displays are being substituted by LED backlights due to the lower power consumption and the wider color gamuts they can offer because of the use of saturated primaries [121,122]. LEDs also have some drawbacks, mainly the instability of their emission curves, which can change with temperature, aging or degradation; color non-uniformity correction circuits are needed for correct color calibration in these displays

[123–125]. Seetzen et al. [126] presented a calibration technique for HDR displays to help overcome degradation problems of the LEDs that cause undesirable color variations in the display over time. Their technique can additionally be modified to extend it to conventional LCD displays. Within this trend of obtaining more pure primaries, lasers have been proposed as an alternative to LEDs due to their extremely narrow spectral distribution, yielding displays that can cover the gamuts of the most common color spaces (ITU-R BT.709, Adobe RGB) [127], or a display offering a color gamut that is up to 190% the color gamut of ITU-R BT.709 [128–131].

Multiple primary displays result in a color gamut that is no longer triangular, and can cover a larger area of the perceivable horseshoe-shaped gamut. Ultra wide color gamut displays using four [132], five [133,134], and up to six color primaries [135–137] have been proposed. Multi-primary displays based on projection also exist [138–141].

3.3. Achieving faithful color reproduction

Tone reproduction operators (see Section 2) can benefit from the application of color appearance models, to ensure that the chromatic appearance of the scene is preserved for different display environments [143]. Several color appearance models (CAMs) have been proposed, with the goal of predicting how colors will be perceived by an observer [144,111,145]. In fact, it has been recently argued that tone reproduction and color appearance, traditionally treated as different problems, could be treated jointly [146] (Fig. 12). Usually, simple post-processing steps are performed to correct for color saturation [66,147]. However, most color appearance models work under a set of simplified viewing conditions; very few, for instance, take into account issues associated with dynamic range. A few notable exceptions exist, such as iCAM [148,149] or the subsequent iCAM06 [150]. Recently, Kim et al. developed a model of color perception based on psychophysical data across most of the dynamic range of the HVS [142] (Fig. 11), while Reinhard and colleagues proposed a model that adapts images and video for specific viewing conditions such as environment illumination or display characteristics [151], as shown in Fig. 13.

From the whole range of colors perceivable by our visual system, only a subset can be reproduced by existing displays. The sRGB color space, which has been the standard for multimedia systems, works well with, e.g., CRT displays but falls short for wider gamut displays. In 2003 the scRGB, an extended RGB color space was approved by the IEC [152], and the extended color space xvYCC [153] followed, which can support a gamut which is nearly double that supported by sRGB.

Faithful color reproduction on devices with different characteristics requires gamut manipulation, known as *gamut mapping*. Gamut mapping can refer both to gamut reduction and expansion, depending on the relationship between the original and target color gamuts [154]; these can further be given by a device or by the content. An example of the latter is the case of image-dependent gamut mapping, where the source gamut is taken from the input image and an optimization is used to compute the appropriate mapping to the target device [155]. Gamut expansion can be done automatically [156,157] or manually by experienced artists. The work of Anderson et al. [158] combines both approaches: an expert expands a single image to meet the target display's gamut and a color transformation is learned from that expansion and applied to each frame of the content. The reader may refer to the work by Muijs et al. [159] and by Laird et al. [160] for a description and evaluation of gamut extension algorithms, or to the comprehensive work of Morovič for a more general view on gamut mapping and color management systems [161]. Finally, the concept of display-adaptive rendering was introduced by Glassner et al. [162], applicable to the inverse case of needing to compress color gamut of content to that of the display. Instead of

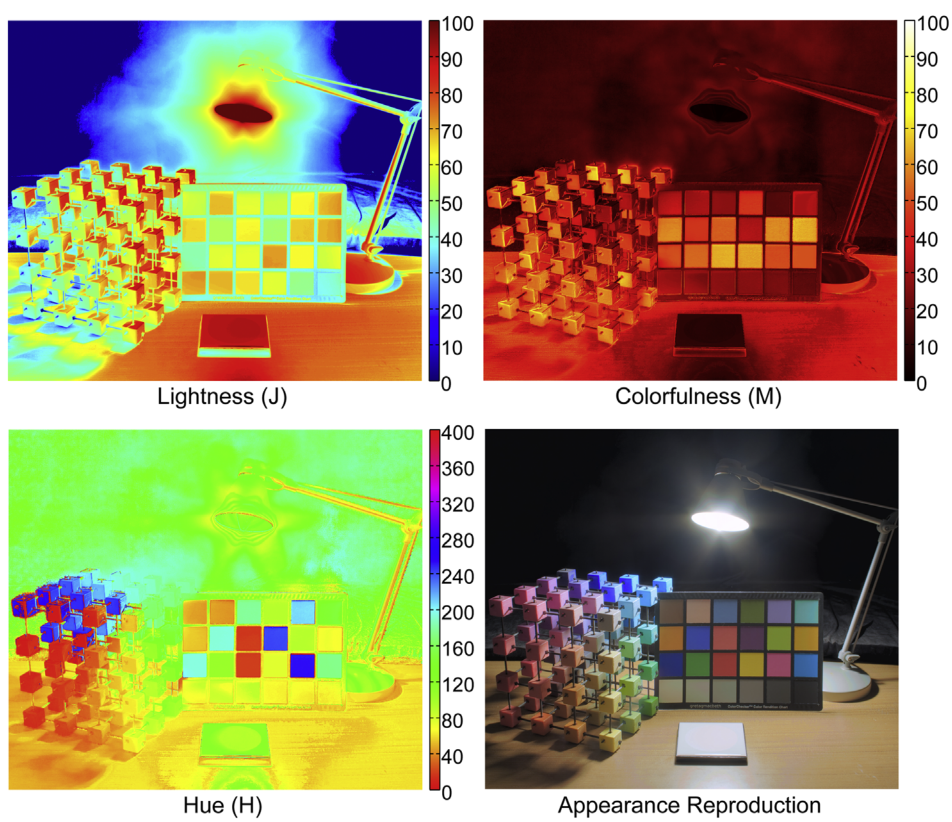

Fig. 11. Color appearance of a high dynamic range image, based on predicted lightness, colorfulness and hue [142] (image copyright ACM 2009). (For interpretation of the references to color in this figure caption, the reader is referred to the web version of this paper.)

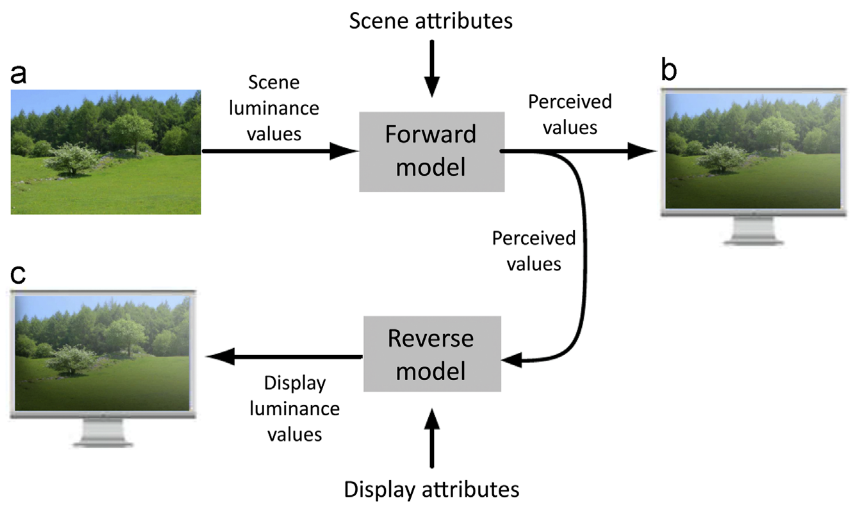

Fig. 12. Typical processing paths for tone reproduction algorithms and color appearance models (CAMs) [146] (image copyright IS&T 2011).

compressing color gamut as a post-process operation on the image [163,164], they propose to automatically modify scene colors so that the rendered image matches the color gamut of the target display.

Accurate reproduction of color is particularly challenging for projection systems, specially if the projection surface properties are unknown and/or the image is not being displayed on a projection-optimized screen. *Radiometric calibration* is required to faithfully display an image in those cases. Typically, projector–camera systems are used for this purpose. This compensation is of special importance in screens with spatially varying reflectance [165,166]. Some authors have incorporated models of the HVS to radiometrically compensate images in a perceptual way, i.e., minimizing *visible* artifacts [167], while others incorporate knowledge of our visual system by computing the differences in perceptually uniform color spaces [168]. Conventional methods usually assume a one-to-one mapping between projector and camera pixels, and ignore global illumination effects, but in the real world there can be surfaces where these effects have a significant influence (e.g., the presence of transparent objects, or complex surfaces with interreflections). Wetzstein and Bimber [169] propose a calibration method which approximates the inverse of the light transport matrix of the scene to perform radiometric calibration in real time and accounting for global illumination effects. These works on radiometric compensation often also deal with geometric correction. Geometric calibration compensates, often by warping the content, for the projection surface being non-planar. An option is to project patterns of structured light onto the scene, as done by, e.g., Zollmann and Bimber [170]; an alternative is to utilize features of the captured distorted projection, first introduced by Yang and Welch [171]. Geometric calibration for projectors is out of the scope of this survey, but we refer the interested reader to the book by Majumder and Brown [15].

4. Improving spatial resolution

High spatial definition is a key aspect when reproducing a scene. It is currently the main factor that displays manufacturers exploit (with terms such as Full HD, HDTV, UHD, referring to different, and not always strictly defined, spatial resolutions of the display), since it has been very well received among customers. So-called 4K displays, i.e., those with a horizontal resolution of around 4000 pixels, are already being commercialized, although producing content at such high resolution has now become an issue due to storage and streaming problems; we describe existing approaches in terms of content generation in Section 4.3.

4.1. Perceptual considerations

Of the two types of photoreceptors in the eye (see Section 2.1), cones have a faster response time than rods, and can perceive finer detail. The highest visual acuity in our retina is achieved in the fovea centralis, a very small area without rods and where the density of cones is largest. According to Nyquist's theorem, assuming a top density of cones in the fovea of 28 arcsec [172], this concentration of cones allows an observer to distinguish one-dimensional sine gratings of a resolution around 60 cycles per degree [173]. Additionally, sophisticated mechanisms of the HVS enhance this resolution, achieving *visual hyperacuity* beyond what the retinal photoreceptors can resolve [174]. In comparison, the pixel size of a typical desktop HD display (a 120 Hz Samsung SyncMaster 2233, 22 in), when viewed at a distance of half a meter, covers approximately nine cones [173]. The peri-foveal region is essentially populated by rods; these are responsible for peripheral vision, which is much lower in resolution. As a consequence, our eyes are only able to resolve with detail the part of a scene which is focused on the fovea; this is one of the reasons for the saccadic movements our visual system performs. Microsaccades are fast involuntary shifts in the gazing direction that our eyes perform during fixation. It is commonly accepted that they are necessary for human vision: if the projection of a stimulus on the retina remains constant the visual percept will eventually fade out and disappear [175].

On the contrary, if the stimulus changes rapidly, the information will be fused in the retina by temporal signal integration [176]. Related to this, the *smooth pursuit eye motion* (SPEM) mechanism in the HVS allows the eyes to track and match velocities with a slowly moving feature in an image [177–179]. This tracking is almost perfect up to 7 deg/s [179], but becomes inaccurate at 80 deg/s [180]. This process stabilizes the image on the retina and allows to perceive sharp and crisp images.

4.2. Display architectures

There is a mismatch between the spatial resolution of today's captured or rendered images, and the resolution that displays that can currently be found in a typical household can show. This effectively means that captured images need to be downsampled

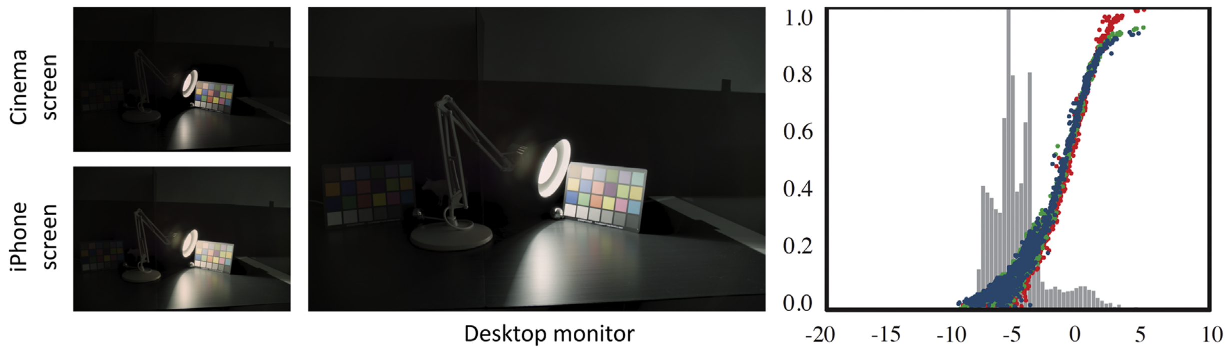

Fig. 13. Accurate color reproduction, taking into account both display type and viewing conditions (shown here for cinema screen, iPhone and a desktop monitor). The plot shows the image histogram in gray, as well as the input/output mapping of the three color channels [151] (image copyright ACM 2012). (For interpretation of the references to color in this figure caption, the reader is referred to the web version of this paper.)

before being shown, which leads to loss of fine details and the introduction of new artifacts. Higher resolution can be achieved by tiling projected images [182–186]. Another obvious way to increase the spatial resolution of displays is to have more pixels per inch, in order to make the underlying grid invisible to the eye. The Retina display by Apple®, for instance, packs about 220 pixels per inch (for a 15 in display). Even though this is a very high pixel density, it is still not enough for a user not to distinguish pixels at the normal viewing distance of 20 in.[1] Other alternatives to a very high pixel density have been explored. With the exception of sub-pixel rendering [187] (Section 4.3), all superresolution displays require specialized hardware configurations. These can be categorized into *optical superposition* and *temporal superposition*.

Optical superposition is a projection principle where low-resolution images from multiple devices are optically superimposed on the projection screen. The superimposed images are all shifted by some amount with respect to each other such that one super-resolved pixel receives contributions from multiple devices. Examples of this technique include [188,189]. Precise calibration of the projection system is essential in these techniques. The optimal pixel states to be displayed by each projector are usually computed by solving a linear inverse problem. Performance metrics for these types of superresolution displays are discussed in [190].

Temporal superposition: Similar to optical superposition techniques, temporal multiplexing requires multiple low-resolution images to be displayed, each shifted with respect to each other. Shown faster than the perceivable flickering frequency of the HVS (which depends on a number of factors, as described in Section 5.1), these images will be fused together by the HVS into a higher resolution one, beyond the actual physical limits of the display. This idea can be seen as the dual of the jittered camera for ensembling a high resolution image from multiple low-resolution versions [192]. The shift can be achieved in single display/projector designs using actuated mirrors [193] or mechanical vibrations of the entire display [181] (Fig. 14). As an interesting avenue of future work, the authors of the latter work outline how the physical vibrations of the display could be avoided, by using a crystal called Potassium Lithium Tantalate Niobate (KLTN), which can change its refractive index [194].

The disadvantage of most existing superresolution displays is that either multiple devices are required, increasing size, weight, and cost of the system, or that mechanically moving parts are necessary. One approach that does not require either is *optical pixel sharing* (OPS) [191,195], which uses two LCD panels and a *jumbling* lens array in projectors to overlay a high-resolution edge image on a coarse resolution image to adaptively increase resolution (Fig. 15). OPS is compressive in the sense that the device does not have the degrees of freedom to represent any arbitrary target image. Much like image compression techniques, OPS relies on the target to be compressible.

4.3. Generation of content

We group existing techniques for higher definition content generation into three categories: superresolution, sub-pixel rendering and temporal integration.

Superresolution: Increasing spatial resolution is related to superresolution techniques (see for instance [196,192,197]). The underlying idea is to take a signal processing approach to reconstruct a higher-resolution signal from a low-resolution one (or several). It is less expensive than physically packing more pixels, and the results can usually be shown on any low-resolution display. Super-resolution techniques are used in different fields like medical imaging, surveillance or satellite imaging. We refer the reader to recent state of the art reports for a complete overview [198,199].

Majumder [200] provides a theoretical analysis investigating the duality between superresolution from multiple captured images, and from multiple overlapping projectors, and shows that superresolution is only feasible by changing the size of the pixels. In their work on display supersampling [188], the authors present a theoretical analysis to engineer the right aliasing in the low-resolution images, so that resolution is increased after superposition, even in the presence of non-uniform grids. The same authors had previously presented a unifying theory of both approaches, tiled and superimposed projection [201].

Sub-pixel rendering: Sub-pixel rendering techniques increase the apparent resolution by taking advantage of the display sub-pixel architecture. Instead of assuming that each channel is spatially coincident, they treat each one differently [202]. This approach has given rise to many different pixel architectures and reconstruction techniques [203–205]. For instance, Hara and Shiramatsu [206] show that an RGGB pattern can extend the apparent pass band of moving images, improving the perceived quality with respect to a standard RGB pattern.

One of the key insights to handle sub-pixel sampling artifacts like color fringes and moire patterns is to leverage the fact that human luminance and chrominance contrast sensitivity functions differ, and both signals can be treated differently. Platt [187] and Klompenhouwer and De Haan [207] exploited this in the context of text rasterization and image scaling, respectively. Platt's method, used in the ClearType functionality, is limited to increased resolution in the horizontal dimension; based on this, other different filtering strategies to reduce color artifacts have been tested [208]. Messing and Daly additionally remove chrominance

[1] Pixel density and viewing distance calculator at http://isthisretina.com/.

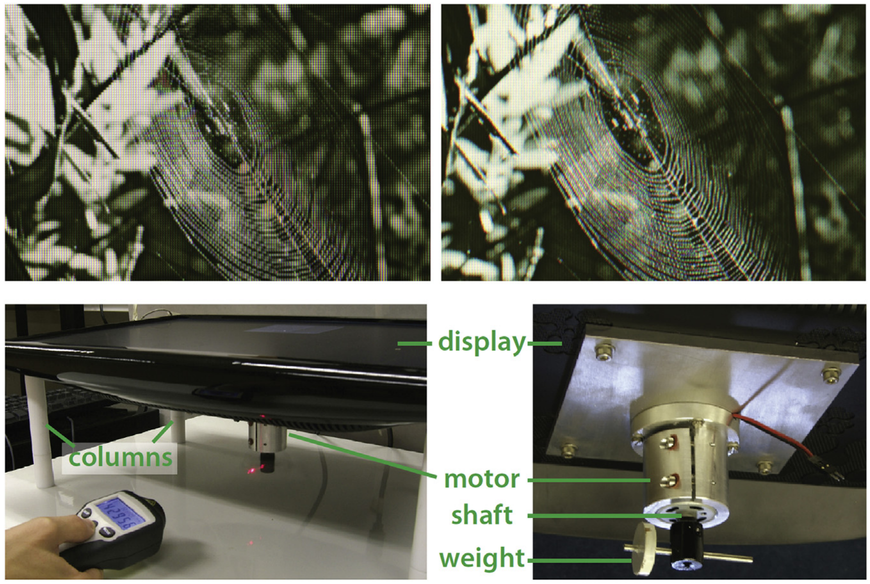

Fig. 14. Spatial resolution enhancement by temporal superposition in a wobbling display. Top left: example image as seen on a conventional (static) display. Top right: higher resolution image perceived on a vibrating display (image credit: Kelsey J. Nelson). Bottom: to vibrate the display, a motor with an offset weight is attached to its back. Centrifugal forces make the screen vibrate as the motor rotates [181] (image copyright ACM 2012).

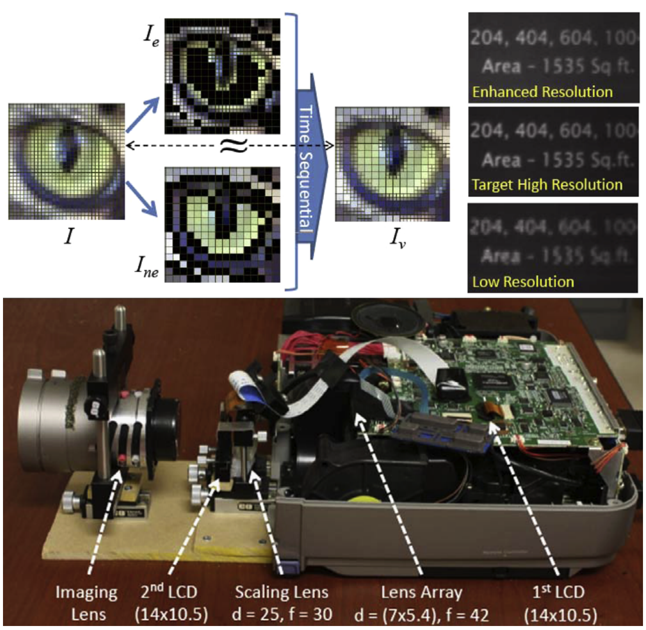

Fig. 15. Spatial resolution enhancement by optical pixel sharing. Top-left: the optical pixel sharing technique decomposes a target high resolution image I into a high resolution *edge* image I_e and a low resolution *non-edge* image I_{ne}, which are then displayed in a time sequential manner to obtain the *edge-enhanced* image I_v. Top-right: comparison of the target image with a low resolution and an enhanced resolution version. Bottom: a side view of the prototype projector, achieving enhanced resolution by cascading two lower-resolution panels [191] (image copyright ACM 2012).

aliasing using a perceptual model [209], while Messing et al. present a constrained optimization framework to mask defective sub-pixels for any regular 2D configuration [210]. These approaches have been recently generalized, presenting optimal, analytical filters for different one- and two-dimensional sub-pixel layouts [211].

Temporal integration: An analysis of the properties of the superimposed images resulting from temporal integration appears in [213]. Berthouzoz and Fattal [181] present an analysis of the theoretical limits of this technique. Instead of physically shaking the display, Basu and Baudisch [214] change the strategy and introduce subtle motion to the displayed images, so that higher resolution is perceived by means of temporal integration. Didyk et al. [212] project moving low resolution images to predictable locations in the fovea, leveraging the SPEM feature of the HVS (see Section 4.1) to achieve perceived high resolution images from multiplexed low resolution content (Fig. 16). This work is limited to one-dimensional, slow panning movements at constant velocity. In subsequent work, the idea is generalized to arbitrary motions and videos, by analyzing the spatially varying optical flow. The assumption is that between consecutive saccades, SPEM closely follows the optical flow [215].

5. Improving temporal resolution

Although spatial resolution is one of the most important aspects of a displayed image, temporal resolution cannot be neglected. In this context, it is crucial that the HVS acts as a time-averaging sensor. This has a huge influence in situations where the displayed signal is not constant over time, or there is motion present in the scene. In this section, we will show that the perceived quality can be significantly affected in such situations and present methods that can improve it.

5.1. Perceptual considerations

The HVS is limited in perceiving high temporal frequencies, i.e., an elevated number of variations in the image per unit time. This is due to the fact that the response of receptors on the retina is not instantaneous [216]. Also, high-level vision processes further lower the sensitivity of the HVS to temporal changes. As a result, temporal fluctuations of the signal are averaged and perceived as a constant signal. One of the basic findings in this field is Bloch's law [217]. It states that the detectability of a stimulus depends on the product of luminance and exposure time. In practice, this means that the perceived brightness of a given stimulus would be the same if the luminance was doubled and the exposure time halved. Although it is often assumed that the temporal integration of the HVS follows this law, it only holds for short duration times (around 40 ms) [217].

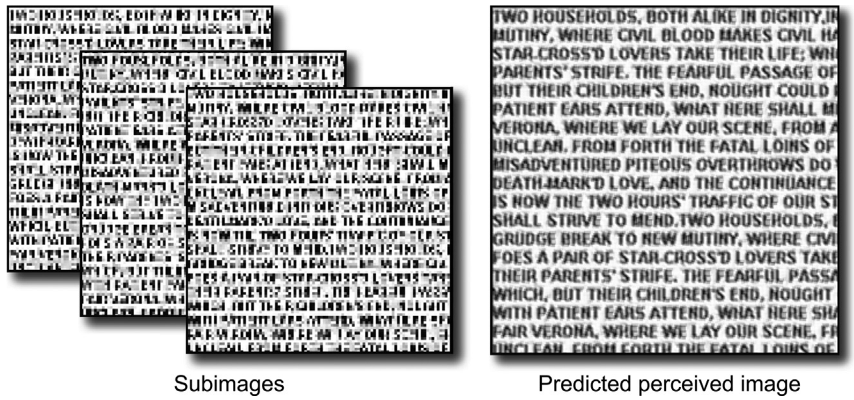

Fig. 16. Spatial resolution enhancement by temporal superposition in a conventional display. Left: low resolution images displayed sequentially in time. Right: corresponding high resolution image perceived as a consequence of the temporal integration performed by the HVS by leveraging SPEM [212] (image copyright ACM 2010).

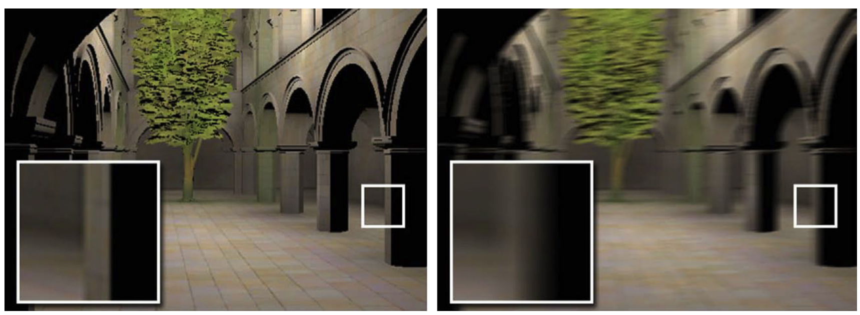

Fig. 17. Simulation of hold-type blur [222]. A user is shown the same animation sequence (sample frame on the left) simultaneously at two different refresh rates. The subject's task is to adjust the blur in the sequence of the right (120 Hz) until the level of blur matches that of the sequence on the left (60 Hz). The average result is shown here: the blurred sequence on the right displayed at 120 Hz is visually equivalent to the sharp sequence on the left displayed at 60 Hz (image copyright Wiley 2010).

From a practical point of view it is more interesting to know when the HVS can perceive temporal fluctuations and when it interprets them as a constant signal. This is defined by the *critical flicker frequency* (CFF) [176], which defines a threshold frequency for a signal to be perceived as constant or as changing over time. The CFF depends on many factors such as temporal contrast, luminance adaptation, retinal region or spatial extent of the stimuli. For different luminance adaptation levels the CFF was measured yielding a temporal contrast sensitivity function [218]. It is also important that the CFF significantly decreases for smaller stimuli, and that peripheral regions of the eretina are more sensitive to flickering [219,220]. Recently, these different factors were incorporated into a video quality metric [221].

In the context of display design, in displays that do not reproduce a constant signal (e.g., CRT displays), low refresh rate can lead to visible and undesired flickering. Another problem that can be caused by poor temporal resolution is jaggy motion. Instead of smooth motion, which is normally observed in the real world, fast moving objects on the screen appear as they were jumping in a discrete way. Also, when the frame rate of the content does not correspond to the frame rate of the display some frames need to be repeated or dropped. This, similar to low frame rate, contributes significantly to reduced smoothness of the motion.

Besides the aforementioned issues, low frame rate may introduce significant blur in the perceived image. This type of blur, often called *hold-type blur*, is purely perceptual and cannot be observed in the content: it arises from the interaction between the display and the HVS [223]. In the real world objects move continuously, and they are tracked by the human eyes almost perfectly; this is enabled by the so-called *smooth pursuit eye motion* (SPEM, refer to Section 4.1 for details). In the context of current display devices, although the tracking is still continuous, the image presented on a screen is kept static for an extended period of time (i.e., the period of one frame). Therefore, due to temporal averaging, the receptors on the retina average the signal while moving across the image during the period of one frame. As a result the perceived image is blurred (see also Fig. 18). The hold-type blur can be modeled using a box filter [224], its support dependent on object velocity and frame rate. This blur is not the same blur as that due to the slow response of the liquid crystals in LCD panels. Pan et al. [223] demonstrated that only 30% of the perceived blur is a consequence of the slow response (and they assumed a response of 16 ms, whereas in current displays this time does not exceed 4 ms). This, together with overdrive techniques, makes the problem of slow response time of displays negligible compared to the hold-type blur. The hold-type blur is a big bottleneck for display manufacturers, as it can destroy the quality of images reproduced using ultra-high resolutions such as 4K or 8K. Since the strength of the blur depends on angular object velocity, the problem becomes even more relevant with growing screen sizes, which are desired in the context of home cinemas or visualization centers.

5.2. Temporal upsampling techniques

A straightforward solution to all problems mentioned above is higher framerate: it reduces jaggy motion and solves the problem of framerate conversion. For higher frame rates the period for which moving objects are kept in the same location is reduced, therefore, it can also significantly reduce hold-type blur. However, high frame rate is not provided in broadcasting applications, and in the context of computer graphics high temporal resolution is very expensive. This forced both the graphics community and display manufacturers to devise techniques to increase the frame rate of the content in an efficient manner.

Fig. 18. Temporal upsampling: the three frames shown in the center have been synthesized from two input images, shown in the leftmost and rightmost images, by moving gradients along a path [232] (image copyright ACM 2009).

Most of the industrial solutions for temporal upsampling that are used in modern TV-sets are designed to compensate for the hold-type blur. Efficiency is key in these solutions, as they are often implemented in small computational units. These techniques usually increase frame rate to, e.g., 100 or 200 Hz, by introducing intermediate frames generated from the low frame rate broadcasted signal.

One of the simplest methods in this context is *black data insertion*, i.e., introducing black frames interleaved with the original content. This solution can reduce hold-type blur because it reduces the time during which the objects are shown in the same position. A similar, more efficient hardware solution is to turn on and off the backlight of LCD panel [223,225]. This is possible because current LCD panels employing LED backlights can switch at frequencies as high as 500 Hz. These two techniques, although fast and easy to implement, suffer from brightness and contrast reduction as well as possible temporal flickering. To overcome these problems, Chen et al. [226] proposed to insert blurred copies of the original frames. Although this ameliorates the brightness issue, it may produce ghosting, since the additional frames are not motion compensated.

More common solutions in current TV screens are *frame interpolation techniques*. In these techniques, additional frames are obtained by interpolating original frames along motion trajectories [227]. Such methods can easily expand a 24 Hz signal, a common standard for movies, to 240 Hz without brightness reduction or flickering. The biggest limitation of these techniques is related to optical flow estimation, which is required for good interpolation. For efficiency reasons simple optical flow techniques are used, which are prone to errors; they usually perform well for slower motions and tend to fail for faster ones [222]. Additionally, these techniques interpolate in-between frames, which requires knowledge of future frames. This introduces a lag which is not a problem for broadcasting applications, but may be unacceptable for interactive applications. In spite of these problems, motion-based interpolation together with backlight flashing is the most common technique in current display devices. An extended survey on these techniques is provided in [225].

An alternative software solution used in TV-sets to reduce hold-type blur is to apply a filtering step which compensates for the blur later introduced by the HVS. This technique is called *motion compensated inverse filtering* [224,228]. In practice, it boils down to applying a 1D sharpening filter oriented along motion trajectories, the blur kernel being estimated from optical flow. The effectiveness of such solution is limited by the fact that the hold-type blur removes certain frequencies which cannot be restored using prefiltering. Furthermore, such techniques are prone to clipping problems and oversharpening.

The problem of increasing temporal resolution is also well known in computer graphics. However, in this area, not all solutions need to provide a real-time performance; for instance some of them were designed to improve low performance of high quality global illumination techniques, where offline processing is not a problem. This, in contrast to previously mentioned industrial solutions, allows for more sophisticated and costly techniques. Another advantage of computer graphics solutions is that they very often rely on additional information that is produced along with the original frames, e.g., depth or motion flow. All this significantly improves the quality of new frames.

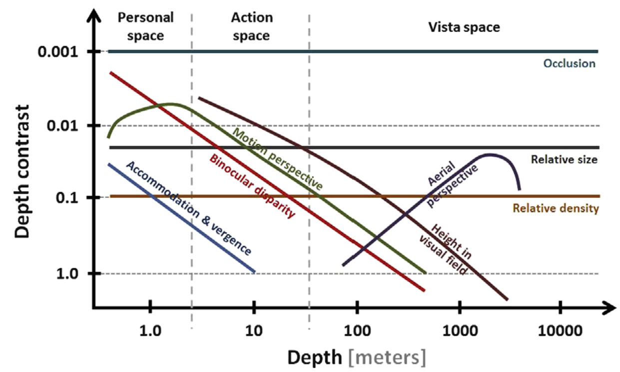

Fig. 19. Sensitivity (just-discriminable depth thresholds) of the HVS to nine different depth cues as a function of distance to the observer. Note that the lower the threshold (depth contrast), the more sensitive the HVS is to that cue. Depth contrast is computed as the ratio of the just-determinable difference in distance between two objects over their mean distance. Adapted from [244].

One group of methods which can be used for creating additional frames and increasing frame rate are *warping techniques*. The idea of these techniques [229] is to morph texture between two target images, creating a sequence of interpolated images; an extended survey discussing these techniques was presented by Wolberg [230]. Recently Liu et al. [231] presented content-preserving warps for the purpose of video stabilization. Using their technique they can synthesize images as if they were taken from nearby viewpoints. This allows them to create video sequences where the camera path is smooth, i.e., the video is stabilized. Although warping techniques were not originally designed for the purpose of improving temporal resolution, they can be successfully used in this context, taking advantage of the fact that interpolated images are very similar when performing temporal upsampling. An example of this is a method by Mahajan et al. [232]. Their technique performs well for single disocclusions, yielding high quality results for standard content (Fig. 18). It requires, however, knowledge of the entire sequence, therefore it is not suitable for real-time applications. Although the high quality of interpolated frames is desirable independent of the location, Stich et al. [233] showed that high-quality edges are crucial for the HVS. Based on this observation, they proposed a technique that takes special care of edges, making their movement more coherent and smooth.

For interactive applications, where frame computation costs can limit interactivity, often additional information such as depth or motion flow is leveraged for more efficient and effective frame interpolation. One of the first methods for temporal upsampling for interactive applications was proposed by Mark et al. [234].

They used depth information to reproject shaded pixels from one frame to another. In order to avoid disocclusions they proposed to use two originally rendered frames to compute in-between frames, which significantly decreases the problem of missing information. Similar ideas were used later where re-use of shaded samples was proposed to speed up image generation. In Render Cache, Walter et al. [235] used forward reprojection to scatter the information from previously rendered frames into new ones. Later, forward reprojection was replaced by reversed reprojection [236]. Instead of re-using pixel colors, i.e., the final result of rendering, also intermediate values can be stored and re-used for computation of next frames [237], speeding up the rendering process. Another efficient method for temporal upsampling in the context of interactive applications was proposed by Yang et al. [238]. Their method uses fixed-point iteration to find a correct pixel correspondence between originally rendered views and interpolated ones. Later, this technique was combined with mesh-based techniques by Bowles et al. [239]. The temporal coherence of computer graphics animations was also explicitly exploited by Herzog et al. [240]: they proposed a spatio-temporal upsampling where they not only increased the frame rate, but also the spatial resolution. A more extensive survey on these techniques can be found in [241].

Although techniques developed for computer graphics applications and for TV-sets have slightly different requirements, it is possible to combine these techniques. Didyk et al. [222] proposed a technique which combines blurred frame insertion and mesh-based warping. The method can be performed in a few milliseconds, and the quality is assured by exploring temporal integration of the HVS. The artifacts in generated frames are blurred, and the loss of high frequencies is compensated in the original frames. This solution eliminates artifacts produced by warping techniques as well as blurred frame insertion. Additionally, the technique performs extrapolation instead of interpolation assuming a linear motion. This eliminates the problem of lag, but can create artifacts for a highly nonlinear and very fast motion. The mesh-based temporal upsampling was further improved in [242].

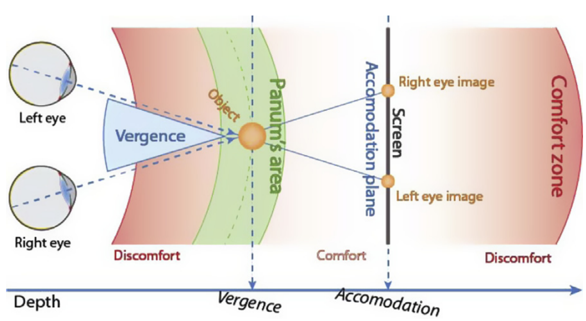

Fig. 20. Accommodation–vergence conflict in stereoscopic displays. While vergence of the eyes is driven to the 3D position of the object perceived, focus (accommodation) remains on the screen. This mismatch can cause fatigue and discomfort to the viewer.

6. Improving angular resolution I: stereoscopic displays

Recently, due to the success of big 3D movie productions, stereo 3D (S3D) is receiving significant attention from consumers as well as manufacturers. This has spurred rapid development in display technologies, trying to bring high quality 3D viewing experiences into our homes. There is also an increasing amount of 3D content available to customers, e.g., 3D movies, stereoscopic video games, even broadcast 3D channels. Despite the fast progress in S3D, there are still many challenging problems in providing perceptually convincing stereoscopic content to the viewers.

6.1. Perceptual considerations

When perceiving the world, the HVS relies on a number of different mechanisms to obtain a good layout perception. These mechanisms, also called depth cues, can be classified as pictorial (e.g., occlusions, relative size, texture density, perspective, shadows), dynamic (motion parallax), ocular (accommodation and vergence) and stereoscopic (binocular disparity) [243]. The sensitivity of the HVS to different cues varies [244], and it depends mostly on the absolute depth. The HVS is able to combine different cues [243, Chapter 5.5.10], which usually strengthen each other; however, in some situations they can also contradict each other. In such cases, the final 3D scene interpretation represents a compromise between the conflicting cues according to their strength. Although much is unknown about cue integration and the relative importance of cues, binocular disparity and motion parallax (see Section 7.1) are argued to be the most relevant depth cues at typical viewing distances [244]. Fig. 19 depicts the influence of depth cues at different distances. A thorough description of all depth cues is outside the scope of this survey, but the interested reader may refer to [245,246] for detailed explanations.

Current 3D display devices take advantage of one of the most appealing depth cues: *binocular disparity*. On such screens the 3D perception is, however, only an illusion created on a flat display by showing two different images to both eyes. In such a case, the conflict between depth cues is impossible to avoid. The most

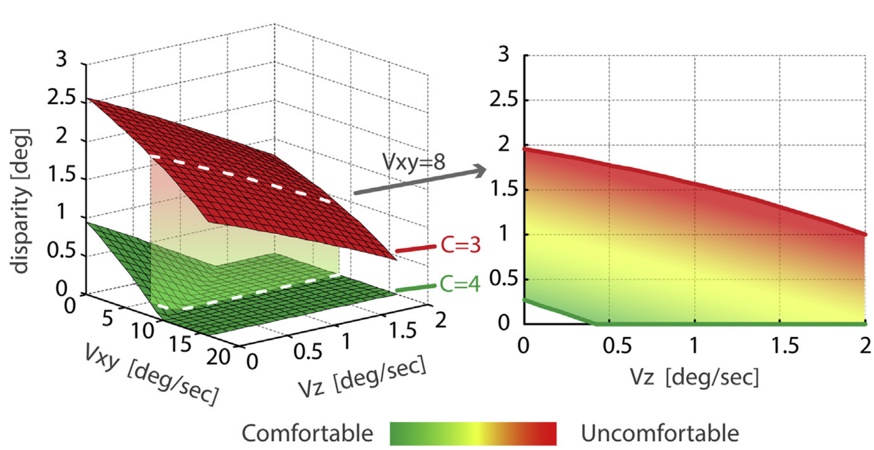

Fig. 21. Example slice of the comfort zone predicted by Du et al., taking into account disparity, motion in depth, motion on the screen plane, and the spatial frequency of luminance contrast [249] (image copyright ACM 2013).

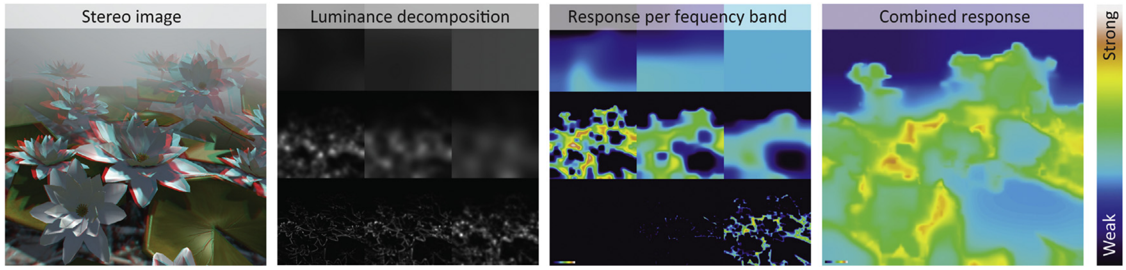

Fig. 22. Perceived disparity as predicted by a recent metric which incorporates the influence of luminance-contrast in the perception of depth from binocular disparity [251]. From left to right: original stereo image, decomposition of the luminance signal into different frequency bands, predicted response of the HVS to the disparity signal for each disparity frequency band separately, and combined response (please refer to the original work for details) (image copyright ACM 2012).

prominent conflict is the *accommodation–vergence mismatch* (Fig. 20). While vergence—the movement the eyes perform for both to foveate the same point in space—can easily adapt to different depths presented on the screen, accommodation—the change in focus of the eyes—tries to maintain the viewed image in focus. When extensive disparities between left and right eye images drive the vergence away from the screen, the conflict between fixation and focus point arises. It can be tolerated up to the certain degree (within the so-called comfort zone), beyond which it can cause visual discomfort [247]. Based on extensive user studies, Shibata et al. [248] derived a model to predict the zone of comfort. Motion is another potential source of discomfort. Recently, Du and colleagues [249] presented a metric of comfort taking into account disparity, motion in depth, motion on the screen plane, and the spatial frequency of luminance contrast (Fig. 21).

The fact that the depth presented on the 3D screen fits into the comfort zone does not yet assure a perfect 3D experience. The retinal images created in the left and right eyes are misaligned, since they originate from different viewpoints. In order to create a clear and crisp image they need to be fused. The HVS is able to perform the fusion only in a region called *Panum's fusional area* (Fig. 20) where relative disparities are not too big; beyond this area double vision (diplopia) is experienced (see e.g., [245, Chapter 5.2]). In fact, binocular fusion is a much complex phenomenon, and it depends on many factors such as individual differences, stimulus properties or exposure duration. For example, people are able to fuse much larger relative disparities for low frequency depth corrugations [250]. The fusion is also easier for stimuli which are well illuminated, have strong texture contrast, or are static.

Assuming that a stereoscopic image is fused by the observer and a single image is perceived, further perception of different disparity patterns depends on many factors. Interestingly, these factors as well as the mechanisms responsible for the interpretation of different disparity stimuli are similar to what is known from luminance perception [252–254]. One of the most fundamental foundings from this field is the contrast sensitivity function (CSF, Section 2.1). Similarly, in depth perception a disparity sensitivity function (DSF) exists. Assuming a sinusoidal disparity corrugation with a given frequency, the DSF function defines a reciprocal of the detection threshold, i.e., the smallest amplitude that is visible to a human observer. Both, CSF and DSF, share the same shape, although the DSF has a peak at a different spatial frequency [254]. Another example of similarities is the existence of different receptive fields tuned to specific frequencies of disparity corrugations [246, Chapter 19.6.3]. Also, similar to luminance perception, apparent depth deduced from the disparity signal is dominated by relative disparities (disparity contrast) rather than absolute depth. Furthermore, illusions which are known from brightness perception exist also for disparity. For example, it turns out that the Craik–O'Brien–Cornsweet illusion (Section 2.1) holds for disparity patterns [255,256]. These similarities suggesting that brightness and disparity perception undergo similar mechanisms have recently been explored to build perceptual models for disparity [257,251] (Fig. 22).

6.2. Display architectures

Since in 1838 Charles Wheatstone invented the first stereoscope, the basic idea for displaying 3D images exploiting binocular disparity has not changed significantly. In the real world, people see two images (left and right eye images), and the same has to be reproduced on the screen for the experience to be similar. Wheatstone proposed to use mirrors which reflect two images located off the side. The observer looking at the mirrors sees these two images superimposed. Wheatstone demonstrated that if the setup is correct, the HVS will fuse the two images and perceive them as if looking at a real 3D scene [258,259].

Since then, people have come up with many different ways of showing two different images to both eyes. The most common method is to use dedicated glasses. A set of solutions employ *spatial multiplexing*: two images are shown simultaneously on the screen, and glasses are used to separate the signal so that each eye sees only one of them. There are different methods of constructing such setup. One possibility is to use different colors for left and right eye (anaglyph stereo). The image on the screen is then composed of two differently tinted images (e.g., red and cyan). The role of the glasses is to filter the signal so a correct image is visible by each eye, using different color filters. Although different filters can be used, due to different colors being shown to both eyes the image quality perceived by the observer is degraded. To avoid it, one can use more sophisticated filters which let through all color components (RGB), but the spectrum of each is slightly shifted and not overlapping to enable easy separation. It is also possible to use polarization to separate left and right eye images. In such solutions, the two images are displayed on a screen with different polarization and the glasses use another set of polarized filters for the separation. Recently, *temporal multiplexing* gained great attention, especially in the gaming community. In this solution, the left and right eye images are interleaved in the temporal domain and shown in rapid succession. The glasses consist of two shutters which can "open and close" very quickly showing the correct image to each eye. A detailed recent review—which also includes head-mounted displays, not covered here—can be found in [260].

Glasses-based solutions have many problems, e.g., reduced brightness, resolution or color shift. However, a bigger disadvantage is the need to wear additional equipment. Whereas this is not a significant problem in movie theaters, people usually do not feel comfortable wearing 3D glasses at home or in other public places. A big hope in this context is glasses-free solutions. So-called *autostereoscopic displays* can show two different images simultaneously, the visibility of which depends on the viewing position. This is usually achieved by placing a parallax barrier or a lenslet array in front of the display panel. We cover these technologies in

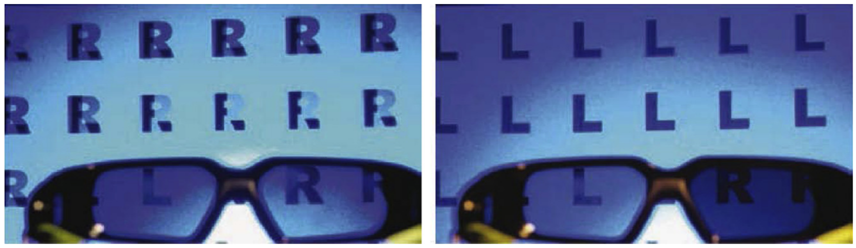

Fig. 23. 3D+2D TV [261]. Left: a conventional glasses-based stereoscopic display: it shows a different view to each eye while wearing glasses, while without glasses both images are seen superimposed. Right: the 3D+2D TV shows a different view to each eye with glasses, while viewers without glasses see one single image, with no ghosting effect (image copyright ACM 2013).

Fig. 24. Left: microstereopsis [268] reduces disparity to the minimum value that would enable 3D perception. Right: backward-compatible stereo [269] aims at preserving the perception of depth in the scene while reducing disparities to enable "standard 2D viewing" (without glasses) of the scene; the Craik–O'Brien–Cornsweet illusion for depth is leveraged in this case to enhance the impression of depth in certain areas while minimizing disparity in others (image copyright IS&T 2012).

detail in Section 7, since the main techniques for autostereoscopic displays can be seen as a particular case of those used for automultiscopic displays.

A stereoscopic version of the content is not always desired by all observers. This can be due to different reasons, e.g., lack of additional equipment, lack of tolerance for such content, or comfort. An interesting problem is thus to provide a solution which enables both 2D and 3D viewing at the same time, the so-called *backward-compatible stereo* [257]. An early approach in this direction was to use color glasses with color filters which minimize ghosting when the content is observed without them; for example, amber and blue filters can be used (ColorCode 3-D). When the 3D content is viewed with the glasses, enough signal is provided to both eyes to create a good 3D perception. However, when the content is viewed without the glasses, the blue channel does not contribute much to the perceived image, and the ghosting is hardly visible. Recently, another interesting hardware solution was provided [261] that improves over the shutter-based solution. Instead of interleaving two images, there is an additional third image which is a negative of one of the two original ones. The 3D glasses are synchronized so that the third image is imperceptible for any eye if the glasses are worn. However, when the observer views the content without the glasses, the third image, due to the temporal integration performed by the HVS (Section 5.1), cancels one of the images of the stereoscopic pair, and only one of them is visible (see Fig. 23).

6.3. Software solutions for improving depth reproduction

In the real world, the HVS can easily adapt to objects at different depths. However, due to the fundamental limitations of stereoscopic displays, it is not possible to reproduce the same 3D experience on current display devices. Therefore, a special care has to be taken while preparing content for a stereoscopic screen. Such content needs to provide a compelling 3D experience, while maintaining viewing comfort. A number of methods have been proposed to perform this task efficiently. The main goal of all these techniques is to fit the depth range spanned by the real scene to the comfort zone of a display device, which highly depends on the viewing setup [248] (e.g., viewing distance, screen size, etc.). This can be performed at different stages of content creation, i.e., during capture or in a post-processing step.

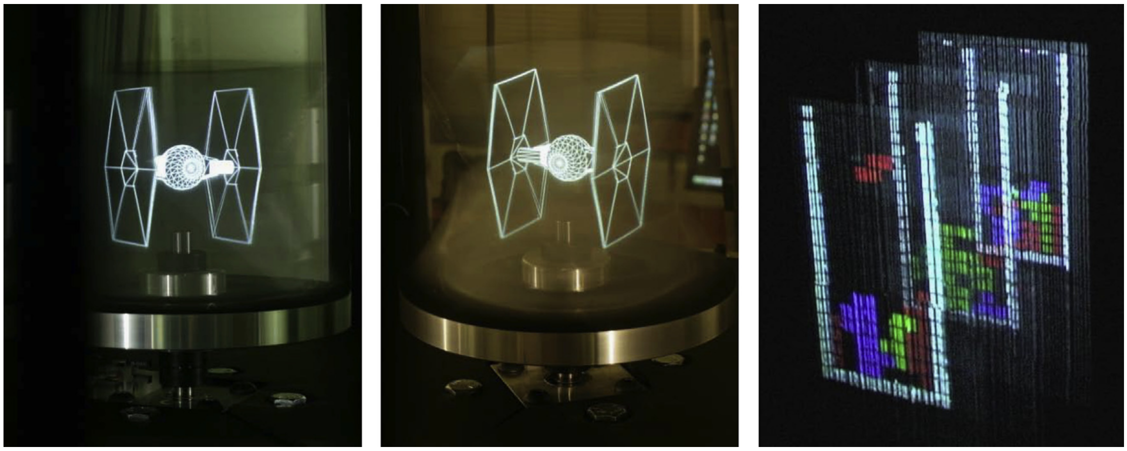

Fig. 25. Two examples of automultiscopic displays. Left: sweeping-based light field display supporting occlusions and correct perspective [280] (TIE fighter copyright LucasArts). Right: volumetric display employing water drops as a projection substrate, here showing an interactive Tetris game [281] (image copyright ACM 2010).

The first group of methods which enables stereoscopic content adjustment are techniques that are applied during the capturing stage. The adjustments are usually performed by changing camera parameters, i.e., interaxial distance—the distance between cameras—and convergence—the angle between the optical axes of the cameras. Changing the first one affects the disparity range by either expanding it or reducing it (smaller interaxial distances result in smaller disparity ranges). The convergence, on the other hand, is responsible for the relative positioning of the scene with respect to the screen plane. Jones et al. [262] proposed a mathematical framework defining the exact modification to camera parameters that need to be applied in order to fit the scene into the desired disparity range. More recently, Oskam et al. [263] proposed a similar approach for real-time applications in which they formulated the problem of camera parameters adjustment as an optimization framework. This allowed them not only to fit the scene into a given disparity range but also to take into account additional artists' design constraints. Apart from that, they also demonstrated how to deal with temporal coherence of such manipulations in real-time scenarios. An interesting system was presented by Heinzle et al. [264]. Their complete camera rig provides an intuitive and easy-to-use interface for controlling stereoscopic camera parameters; the interface collects high-level feedback from the artists and adjusts the parameters automatically. In practice, it is also possible to record the content with multiple camera setups, e.g., a different one for background and foreground, and the different video streams combined during the compositing stage. A big advantage of techniques which directly modify the camera parameters is that they can also compensate for object distortions arising from the wrong viewing position [265].

The aforementioned methods are usually a satisfactory solution if the viewing conditions are known in advance. However, in many scenarios, the content captured with a specific camera setup, i.e., designed for a particular display, is also viewed on different screens. To fully exploit the available disparity range, post-processing techniques are required to re-synthesize the content as if it were captured using different camera parameters. Such *disparity retargeting* methods usually work directly on disparity maps to either compress or expand disparity range. An example of such techniques was presented by Lang et al. [266]. By analogy to tone-mapping operators (Section 2.3), they proposed to use different mapping curves to change the disparity values. The mapping can be done according to differently designed curves (e.g., linear or logarithmic curves). It can also be performed in the gradient domain. In order to improve depth perception of important objects, they also proposed to incorporate saliency prediction into the curve design. The problem of computing adjusted stereo images is formulated as an optimization process that guides a mesh-based warp according to the edited disparity maps. It is also possible to use more explicit methods which do not involve optimization [242].

Recently, perceptual models for disparity have been proposed [257,251]. With their aid, disparity values can be transformed into a perceptually uniform space, where they can be mapped to fit a desired disparity range. Essentially, the disparity range is reduced while preserving the disparity signal whenever it is most relevant for the HVS. Perceptual models of disparity can additionally be used to build metrics which can evaluate perceived differences in depth between an original stereo image and its modified version. This allows for defining the disparity remapping problem as an optimization process where the goal is to fit disparities into a desired range while at the same time minimizing perceived distortions [251]. As the metrics can also account for different luminance patterns, such methods were shown to perform well for automultiscopic displays where the content needs to be filtered to avoid inter-view aliasing [267]. More about adopting content for such screens can be found in Section 7.3. Disparity models also enable depth perception enhancement. For example, when the influence of luminance patterns on disparity perception is taken into account [251], it is possible to enhance depth perception in regions where it is weakened due to insufficient texture. This can be done by introducing additional luminance information.

One of the most aggressive methods for stereo content manipulation is microstereopsis. Proposed by Siegel et al. [268], this technique reduces the camera distance to a minimum so that a stereo image has just enough disparity to create a 3D impression. This solution can be useful in the context of *backward-compatible stereo* because the ghosting artifacts during monoscopic presentation are significantly reduced. Didyk et al. [257,269] proposed another stereo content manipulation technique for backward-compatible stereo. Their method uses the Craik–O'Brien–Cornsweet illusion to reproduce disparity discontinuities. As a result, the technique significantly reduces possible ghosting when the content is viewed without stereoscopic equipment, but a good 3D perception can be achieved when the content is viewed with the equipment. It is also possible to enhance depth impression by introducing Cornsweet profiles atop of the original disparity signal. Fig. 24 shows examples of these techniques.

All aforementioned techniques for stereoscopic content adjustment do not analyze how much such manipulations affect motion perception. Recently, Kellnhofer et al. [270] proposed a technique for preventing visible motion distortions due to disparity manipulations. Besides, previously mentioned techniques are mostly

Fig. 26. Top row: a prototype tensor display. Middle row: two different views of a light field as seen on the tensor display. Bottom row: layered patterns for two different frames [297].

concerned with the disparity signal introduced by scene geometry. However, extensive disparities can also be created by secondary light effects such as reflection. Templin et al. [271] proposed a technique that explicitly accounts for the problem of glossy reflections in stereoscopic content. Their technique prevents viewing discomfort due to extensive disparities coming from such reflections, while maintaining at the same time their realistic look (Fig. 25).

7. Improving angular resolution II: automultiscopic displays

Automultiscopic displays, capable of showing stereo images from different viewpoints without the need to wear glasses or other additional equipment, have been a subject of much research throughout the last century. A recent state-of-the-art review on 3D displays including glasses-free techniques can be found in [260]. We briefly outline these technologies and discuss in more detail the most recent developments on light field displays, both in terms of hardware and of content generation. In this survey, we do not discuss holographic imaging techniques (e.g., [272]), which present all depth cues, but are expensive and primarily restricted to static scenes viewed under controlled illumination [273].

7.1. Perceptual considerations

As discussed in Section 6.1, there is a large number of cues the HVS utilizes to infer the (spatial layout and) depth of a scene (Fig. 19). Here we focus on motion parallax, which is the most distinctive cue of automultiscopic displays, not provided by conventional stereoscopic or 2D displays.

Motion parallax enables us to infer depth from relative movement. Specifically, it refers to the movement of an image projected in the retina as the object moves relative to the viewer; this movement is different depending on the depth at which the object is with respect to the viewer, and the velocity of the relative motion. Depth perception from motion parallax exhibits a close relationship in terms of sensitivity with that of binocular disparity, suggesting similar underlying processes for both depth cues [274,275]. Existing studies on sensitivity to motion parallax are not as exhaustive as those on disparity, although several experiments have been conducted to establish motion parallax detection thresholds [276]. The integration of both cues, although still largely unknown, has been shown to be nonlinear [277].

Consistent vergence–accommodation cues and motion parallax are required for a natural comfortable 3D experience [278]. Automultiscopic displays, potentially capable of providing these cues, are emerging as the new generation of displays, although limitations persist, as discussed in the next subsection. Additional issues that may hinder the viewing experience in automultiscopic displays are crosstalk between views, moire patterns, or the cardboard effect [278,279].

7.2. Display architectures

Volumetric displays: Blundell and Schwartz [282] define a volumetric display as permitting "the generation, absorption, or scattering of visible radiation from a set of localized and specified regions within a physical volume". Many volumetric displays exploit high-speed projection synchronized with mechanically rotated screens. Such swept volume displays were proposed as early as 1912 [283] and have been continuously improved [284]. Designs include the Seelinder [285], exploiting a spinning cylindrical parallax barrier and LED arrays, and the work of Maeda et al. [286], utilizing a spinning LCD panel with a directional privacy filter. Several designs have eliminated moving parts using electronic diffusers [287], projector arrays [288], and beam-splitters [289]. Whereas others consider projection onto transparent

Fig. 27. Progressive reconstruction of a light field by adaptive image synthesis. In can be seen in the close-ups how the cumulative light field samples used represent a very sparse set of all plenoptic samples [311] (image copyright ACM 2013).

substrates, including water drops [281] (Fig. 26, right), passive optical scatterers [290], and dust particles [291].

Light field displays: Light field displays generally aim to create motion parallax and stereoscopic disparity so that an observer perceives a scene as 3D without having to wear encumbering glasses. Invented more than a century ago, the two fundamental principles underlying most light field displays are parallax barriers [2] and integral imaging with lenslet arrays [292]. The former technology has evolved into fully dynamic display systems supporting head tracking and view steering [293,294], as well as high-speed temporal modulation [295]. Today, lenslet arrays are often used as programmable rear-illumination in combination with a high-speed LCD to steer different views toward tracked observers [296]. Not strictly a volumetric display, but also based on a spinning display surface, Jones et al. [280] instead achieve a light field display (Fig. 26, left) which preserves accurate perspective and occlusion cues, often not present in volumetric displays. The display utilizes an anisotropic diffusing screen and user tracking, and exhibits horizontal parallax only.

Compressive light field displays: Through the co-design of display optics and computational processing, compressive displays strive to transcend limits set by purely optical designs. It was recently shown that tomographic light field decompositions displayed on stacked films of light-attenuating materials can create higher resolutions than previously possible [298]; and the same underlying approach later applied to stacks of LCDs for displaying dynamic content [299]. A compression is achieved in the number of layer pixels, which is significantly smaller than the number of emitted light rays. Low-rank light field synthesis was also demonstrated for dual-layer [295] and multi-layer displays with directional backlighting [297]. In these display designs, an observer perceptually averages over a number of patterns (shown in Fig. 26 for a so-called tensor display) that are displayed at refresh rates beyond the critical flicker frequency of the HVS (see Section 5.1). The limited temporal resolution of the HVS is directly exploited by decomposing a target light field into a set of patterns, by means of nonnegative matrix or tensor factorization, and presenting them on high-speed spatial light modulators; this creates a perceived low-rank approximation of the target light field.

Light field displays supporting accommodation: Displays supporting correct accommodation are able to create a light field with enough angular resolution to allow subtle, yet crucial, variation over the pupil. Such displays utilize three main approaches. Ultra-high angular resolution displays, such as super-multiview displays [300–302] (Fig. 29), take a brute-force approach: all possible views are generated and displayed simultaneously, incurring high hardware costs. In practice, this has limited the size, field of view, and spatial resolution of the devices. Multi-focal displays [289,303,304] virtually place conventional monitors at different depths via refractive optics. This approach is effective, but requires encumbering glasses. Volumetric displays [283,280,284] also support accommodative depth cues, but usually only within the physical device; current volumetric approaches are not scalable past small volumes. Most recently a compressive accommodation display architecture was proposed [305]. This approach is capable of generating near correct accommodation cues with high spatial resolution over a wide field of view using multi-layer display configurations that are combined with high angular resolution backlighting and driven by nonnegative light field tensor factorizations. Finally, Lanman and Luebke recently presented a near-eye light field display capable of presenting accommodation, convergence, and binocular disparity depth cues; it is a head-mounted display (HMD) with a thin form-factor [306].

7.3. Image synthesis for automultiscopic displays

Stereoscopic displays pose a challenge in what regards to content generation because of the need to capture or render two views, the positioning of the cameras or the content post-processing (Section 6.3). Multiview content shares these challenges, augmented by additional issues derived from the size of the input data, the computation needed for image synthesis, and the intrinsic limitations that these displays exhibit.

Although targeted to parallax barriers and lenslet array displays, Zwicker et al. [267] were one of the first to address the problem of reconstructing a captured light field to be shown on light field displays, building on previous work on plenoptic sampling [307,308]. They proposed a resampling filter to avoid the aliasing derived from limited angular resolution, and derived optimal camera parameters for acquisition.

Ranieri et al. [309] propose an efficient rendering algorithm for multi-layer automultiscopic displays which avoids the need for an optimization process, common in compressive displays. The algorithm is simple, essentially assigning each ray to the display layer closest to the origin and then filtering for antialiasing; they have to

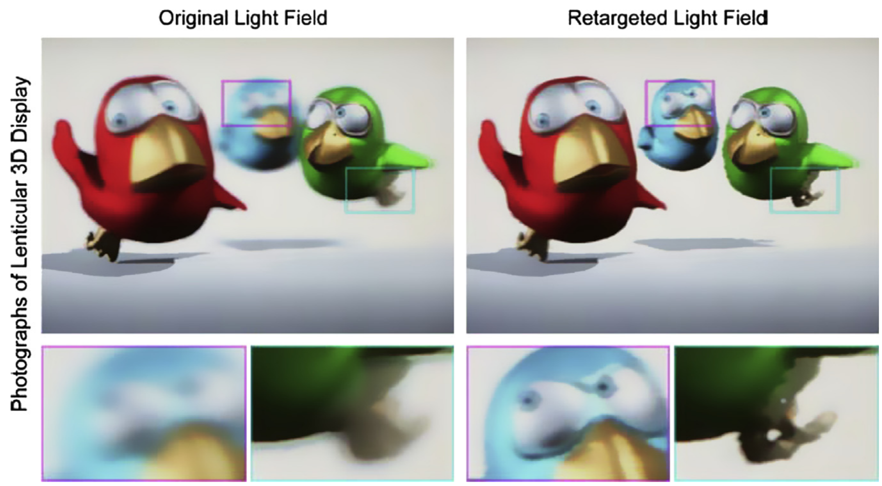

Fig. 28. 3D content retargeting for automultiscopic displays allows for a sharp representation of the images within the depth budget of the display, while retaining the original sensation of depth [314].

Fig. 29. Tailored displays can enhance visual acuity. For each scene, from left to right: input image, images perceived by a farsighted subject on a regular display, and on a tailored display [302] (image copyright ACM 2012).

assume, however, depth information of the target light field to be known. Similar to this algorithm, but generalized to an arbitrary number of emissive and modulating layers, and with a more sophisticated handling of occlusions, is the decomposition algorithm for rendering light fields in [310].

Compressive displays, described in Section 7.2, typically require taking a target 4D light field as input and solving an optimization problem for image synthesis. This involves a large amount of computation, currently unfeasible in real time for high angular and spatial resolutions. To overcome the problem, Heide et al. [311] recently proposed an adaptive optimization framework which combines the rendering and optimization of the light field into a single framework. The light field is intelligently sampled leveraging display-specific limitations and the characteristics of the scene to be displayed, allowing to significantly lower computation time and bandwidth requirements (see Fig. 27). The method is not limited to compressive multiview displays, but can also be applied to high dynamic range displays or high resolution displays.

In the production of stereo content, a number of techniques exist that generate a stereo pair from a single image. This idea has been extended to automultiscopic displays, Singh and colleagues [312] propose a method to generate, from existing stereo content, the patterns to display in a glasses-free two-layer automultiscopic display to create the 3D effect. Their main contribution lies in the stereo matching process (performed to obtain a disparity map), specially tailored to the characteristics of a multi-layer display to achieve temporal consistency and accuracy in the disparity map. Depth estimation can, however, be a source of artifacts with current methods. To overcome this problem, Didyk et al. [313] proposed a technique that expands a standard stereoscopic content to a multi-view stream avoiding depth estimation. The technique combines both, view synthesis and filtering for antialiasing into one filtering step. The method can be performed very efficiently, reaching a real-time performance.

Content retargeting refers to the algorithms and methods that aim at adapting content generated for a specific display to another display that may be different in one or more dimensions: spatial, angular or temporal resolution, contrast, color, depth budget, etc. [315,316]. An example in automultiscopic displays is the first spatial resolution retargeting algorithm for light fields, proposed by Birklbauer and Bimber [317]; it is based on seam carving and does not require knowing or computing a depth map of the scene. *Disparity retargeting* for stereo content is discussed in Section 6.3. Building on this literature on retargeting of stereo content, a number of approaches have emerged that perform disparity remapping on multiview content (light fields). The need for these algorithms can arise from viewing comfort issues, artistic decisions in the production pipeline, or display-specific limitations. Automultiscopic displays exhibit a limited depth-of-field which is a consequence of the need to filter the content to avoid inter-view aliasing. As a result, the depth range within which images can be shown appearing sharp is constrained, and depends on the type and characteristics of the display itself: depth-of-field expressions have been derived for different types of displays [267,298,297].

One of the first to address depth scaling in multiview images were Kim et al. [318]. Given the multiview images and the target scaled depth, their algorithm warps the multiview content and performs hole filling whenever disocclusions are present. More sophisticated is the method by Kim and colleagues for manipulating the disparity of stereo pairs given a 3D light field (horizontal parallax only) of the scene [319]. They build an EPI (epipolar-plane image) volume, and compute optimal cuts through it based on different disparity remapping operators. Cuts correspond to images with multiple centers of projection [320], and the method can be applied both to stereo pairs and to multiview images, by performing two or more cuts through the volume according to the corresponding disparity remapping operator. As an alternative, perceptual models for disparity which have recently been developed [257,251] can also be applied to disparity remapping for automultiscopic displays. This is explained in more detail in Section 6.3, but essentially these models allow to leverage knowledge on the sensitivity to disparity of the HVS to fit disparity into the constraints imposed by the display. Leveraging Didyk et al.'s model [257], together with a perceptual model for contrast sensitivity [321], and incorporating display-specific depth-of-field functions, Masia et al. [322,314] propose a retargeting scheme for addressing the trade-off between image sharpness and depth perception in these displays (Fig. 28).

7.4. Applications

In this subsection, we discuss additional applications of light field displays: human computer interaction and vision-correcting image display.

Interactive light field displays: Over the last few years, interaction capabilities with displays have become increasingly important. While light field displays facilitate glasses-free 3D displays where virtual objects are perceived as floating in front of and behind the physical device, most interaction techniques focus on either on-screen (multi-touch) interaction or mid-range and far-range gesture-based interaction facilitated by computational photography techniques, such as depth-sensing cameras, or depth-ranging sensors like Kinect™. Computational display approaches to facilitating mid-range interaction have been proposed. These integrate depth sensing pixels directly into the screen of a light field display by splitting the optical path of a conventional lenslet-based light field display such that a light field is emitted and simultaneously recorded through the same lenses [323,324]. Alternatively, light field display and capture mode can be multiplexed in time using a high-speed liquid crystal panel as a bidirectional 2D display and a 4D parallax barrier-based light field camera [325].

Vision-correcting displays: Light field displays have recently been introduced for the application of correcting the visual aberrations of an observer (Fig. 29). Early approaches attempt to filter a 2D image presented on a conventional screen with the inverse point spread function (PSF) of the observer's eye [326–328]. Although these methods slightly improve image sharpness, contrast is reduced; fundamentally, the PSF of an eye with refractive errors is a low-pass filter—high image frequencies are irreversibly canceled out in the optical path from display to the retina. To overcome this limitation, Pamplona et al. [302] proposed the use of conventional light field displays with lenslet arrays or parallax barriers to correct visual aberrations. For this application, these devices must provide a sufficiently high angular resolution so that multiple light rays emitted by a single lenslet enter the pupil. This resolution requirement is similar for light field displays supporting accommodation cues. Unfortunately, conventional light field displays as used by Pamplona et al. [302] are subject to a spatio-angular resolution tradeoff: an increased angular resolution decreases the spatial resolution. Hence, the viewer sees a sharp image but at a significantly lower resolution than that of the screen. To mitigate this effect, Huang et al. [329] recently proposed to use multi-layer display designs together with prefiltering. While this is a promising, high-resolution approach, combining prefiltering and these particular optical setups significantly reduces the resulting image contrast.

8. Conclusion and outreach

We have presented a thorough literature review of recent advances in display technology, categorizing them along the multiple dimensions of the plenoptic function. Additionally, we have introduced the key aspects of the HVS that are relevant and/or leveraged by some of the new technologies. For readers also seeking an in-depth look into hardware descriptions, domain-specific books exist covering aspects such as physics or electronics, particular technologies like organic light-emitting diode (OLED), liquid crystal, LCD backlights or mobile displays [10,11], or even how to build prototype compressive light field displays [330].

Advances in display technologies run somewhat parallel to advances in *capture* devices: exploiting the strong correlations between the dimensions of the plenoptic function has allowed researchers and engineers to overcome basic limitations of standard capture devices. Examples of these include color demosaicing, or video compression [47]. The fact that both capture and display technologies are following similar paths makes sense, since both share the problem of the high dimensionality of the plenoptic function. In this regard, both fields can be seen as two sides of the same coin. On the other hand, advances in one will foster further research in the other: for instance, HDR displays have already motivated the invention of new HDR capture and compression algorithms, which in turn will create a demand for better HDR displays. Similarly, a requirement for light field displays to really take off is that light field content becomes more readily available (with companies like Lytro™ and Raytrix™ pushing in that direction).

Our categorization in this survey with respect to the plenoptic function is a convenient choice to support our current view of the field, but it should not be seen as a rigid scheme. We expect this division to become increasingly blurrier over the next few years, as some of the most novel technologies mature, coupled with superior computational power and a better knowledge of the HVS. The most important criteria nowadays for the consumer market seem to be spatial resolution, contrast, angular resolution (3D) and refresh rates.

High definition (ultra-high spatial resolution) is definitely one of the main current trends in the industry. A promising technology is based on IGZO (Indium Gallium Zinc Oxide), a transparent amorphous oxide semiconductor (TAOS) whose TFT (Thin Film Transistor) performance increases electron mobility up to a factor of 50. This can lead to an improvement in resolution of up to ten times, plus the ability to fabricate larger displays [331]. Additionally, TAOS can be flexed, and have a lower consumption of power during manufacturing, because they can be fabricated at room temperature. The technology has already been licensed by JST (the Japan Science and Technology Agency) to several display manufacturing companies.

Other technologies have their specific challenges to meet before they become the driving force of the industry towards the consumer market. In the case of increased contrast, power consumption is one stumbling block for HDR displays, also shared by some types of automultiscopic displays. LCD panels transmit about 3% of light for pixels that are full on, which means that a lot of light is transduced into heat. For HDR displays, this translates into lots of energy consumed and wasted. OLED technology is a good candidate as a viable, more efficient technology. In the case of automultiscopic displays, parallax barriers entail very low light throughput as well, whereas LCD-based multi-layer approaches multiply the efficiency problem times the number of LCD panels needed. While the field is very active, major challenges of automultiscopic displays that remain and have been discussed in this review include the need for a thin form factor, a solution to the currently still low spatio-angular resolution, limited depth of field, or the need for easier generation and transmission of the content.

While we have shown the recent advances and progress lines in each plenoptic dimension, we believe that real advances in the field need to come from a holistic approach to the problem: instead of focusing on one single dimension of the plenoptic function, future displays need to and will tackle several dimensions at the same time. For instance, current state-of-the-art broadcast systems achieve Ultra High Definition (UHD) with 8K at 120 Hz progressive, with a deeper color gamut (Rec. 2020) than High Definition standards. This represents a significant advance in terms of spatial resolution, temporal resolution, and color. Similarly, we have seen how dynamic range and color appearance models, formerly two separate fields, are now being analyzed in conjunction in recent works, or how fast changes in the temporal domain can help increase apparent spatial resolution. Stereo techniques can be seen as just a particular case of automultiscopic displays, and these need to analyze spatial and angular resolution jointly. Joint stereoscopic high dynamic range displays (SHDR, also known as 3D-HDR) are also being developed and studied. This is the trend for the future.

As technology advances, some of the inherent limitations of current displays (such as bandwidth in the case of light field displays) will naturally vanish, or progressively become less restricting. However, while some advances will rely purely on novel technology, optics and computation, we believe that perceptual aspects will continue to play a key role. Understanding the mechanisms of the HVS will be a crucial factor on which design decisions will be taken. For instance, SHDR directly involves the luminance contrast and angular dimensions of the plenoptic function. However, the perception of depth in high dynamic range displays is still not well known; some works have even hypothesized that HDR content may hinder stereo acuity [332]. In any case it is believed that the study of binocular disparity alone, on which most of the existing research has focused, is not enough to understand the perception of a 3D structure [333]. Although we are gaining a more solid knowledge on how to combat the vergence–accommodation conflict, or what components in a scene may introduce discomfort to the viewer, key aspects of the HVS such as cue integration, or the interrelation of the different visual signals, remain largely unexplored. As displays become more sophisticated and advanced, a deeper understanding of our visual system will be needed, including hard-to-measure aspects such as viewing comfort.

Last, a different research direction which has seen some first practical implementations aims at integrating the displayed imagery with the physical world, blurring out the boundaries imposed by the form factors of more traditional displays. Examples of this include systems that augment the appearance of objects by means of superimposed projections [334,335]; compositing real and synthetic objects in the same scene, taking into account interreflections between them [336]; adjusting the appearance of the displayed content according to the incident real illumination [337]; or allowing for gestured-based interaction [325]. Some of these approaches rely on the integration and combined operation of displays, projectors and cameras, all of them enhanced with computational capabilities. This is another promising avenue of future advances, although integrating hardware from different manufacturers may impose some additional practical difficulties. Another exciting, recent technology is *printed optics* [338,339], which enables display, sensing and illumination elements to be directly printed inside an interactive device. While still in its infancy, this may open up a whole new field, where every object will in the future act as a display.

To summarize, we believe that future displays will rely on joint advances on several different dimensions. Additional influencing factors include further exploration of aspects such as polarization, or multispectral imaging; new materials; the adaptation of mathematical models for high-performance real-time computation; or the co-design of custom optics and electronics. We are convinced that a deeper understanding of the HVS will play a key role as well, with perceptual effects and limitations being taken into account in future display designs. Display technology encompasses a very broad field which will benefit from close collaboration from the different areas of research involved. From hardware specialists to psychophysicists, including optics experts, material scientists, or signal processing specialists, multidisciplinary co-operation will be the key.

Acknowledgments

We would like to thank the reviewers for their valuable feedback, and Erik Reinhard for his insightful comments on HDR imaging. We would also like to thank Robert Simon for sharing the photographs of the double portrait, as well as the authors who granted us permission to use images from their techniques. This research has been funded by the EU through the projects GOLEM (grant no.: 251415) and VERVE (grant no.: 288914). Belen Masia was additionally funded by an FPU grant from the Spanish Ministry of Education and by an NVIDIA Graduate Fellowship. Gordon Wetzstein was supported by an NSERC Postdoctoral Fellowship.

References

[1] Simon R. Gaspar Antoine de Bois-Clair. Robert Simon fine art. ⟨http://www.robertsimon.com/pdfs/boisclair_portraits.pdf⟩; 2013.
[2] Ives FE. Parallax stereogram and process of making same. U.S. Patent 725, 567; 1903.
[3] Lippmann G. La photographie intégrale. Acad Sci 1908;146:446–51.
[4] Adelson E, Bergen J. The plenoptic function and the elements of early vision. In: Computational models of visual processing, vol. 1, 1991. p. 3–20.
[5] Bimber O, Iwai D, Wetzstein G, Grundhöfer A. The visual computing of projector–camera systems. In: ACM SIGGRAPH 2008 classes. SIGGRAPH '08. New York, NY, USA: ACM; 2008. p. 84:1–25.
[6] Holliman N, Dodgson N, Favalora G, Pockett L. Three-dimensional displays: a review and applications analysis. IEEE Trans Broadcast 2011;57(2):362–71.
[7] Benton SA, editor. Selected papers on three-dimensional displays. SPIE Press; 2001.
[8] Wetzstein G, Lanman D, Gutierrez D, Hirsch M. Computational Displays: combining optical fabrication, computational processing, and perceptual tricks to build the displays of the future. ACM SIGGRAPH Course Notes; 2012.
[9] Wetzstein G, Lanman D, Didyk P. Computational displays. In: Eurographics 2013 tutorials, 2013.
[10] Lueder E. 3D displays. Wiley series in display technology. 1st ed.Wiley; 2012.
[11] Hainich RR, Bimber O. Displays: fundamentals and applications. CRC Press/A. K. Peters; 2011.
[12] Grosse M, Wetzstein G, Grundhöfer A, Bimber O. Coded aperture projection. ACM Trans Graph 2010 22:1–12.
[13] Ma C, Suo J, Dai Q, Raskar R, Wetzstein G. High-rank coded aperture projection for extended depth of field. In: International conference on computational photography (ICCP), 2013.
[14] Bimber O, Raskar R. Spatial augmented reality: merging real and virtual worlds. A K Peters/CRC Press; 2005 ISBN 978-1568812304.
[15] Majumder A, Brown MS. Practical multi-projector display design. Natick, MA, USA: A. K. Peters Ltd.; 2007 ISBN 1568813104.
[16] Reinhard E, Ward G, Pattanaik SN, Debevec PE, Heidrich W. High dynamic range imaging—acquisition, display, and image-based lighting. 2nd ed. Academic Press; 2010 ISBN 9780123749147.
[17] Debevec PE. Image-based lighting. IEEE Comput Graph Appl 2002;22 (2):26–34.
[18] Khan EA, Reinhard E, Fleming RW, Bülthoff HH. Image-based material editing. ACM Trans Graph 2006;25(3):654–63.
[19] Bimber O, Iwai D. Superimposing dynamic range. ACM Trans Graph 2008;27 (5).
[20] Banterle F, Artusi A, Debattista K, Chalmers A. Advanced high dynamic range imaging: theory and practice. AK Peters, CRC Press; 2011 ISBN 9781568817194.
[21] Hoefflinger B. High-dynamic-range (HDR) vision: microelectronics, image processing, computer graphics. Springer series in advanced microelectronics. Secaucus, NJ, USA: Springer-Verlag New York Inc.; 2007 ISBN 3540444327.
[22] Myszkowski K, Mantiuk R, Krawczyk G. High dynamic range video. Morgan & Claypool Publishers; 2007 ISBN 1598292145.
[23] Aydın T. Human visual system models in computer graphics [Ph.D. thesis]. Max Planck Institute for Computer Science; 2010.
[24] Xiao F, DiCarlo J, Catrysse P, Wandell B. High dynamic range imaging of natural scenes. In: The Tenth color imaging conference, 2002.
[25] Wandell BA. Foundations of vision. Sinauer Associates Inc.; 1995 ISBN 9780878938537.
[26] Mather G. Foundations of perception. Psychology Press; 2006 ISBN 9780863778346.
[27] Fain GL, Matthews HR, Cornwall MC, Koutalos Y. Adaptation in vertebrate photoreceptors. Physiol Rev 2001;81(1):117–51.
[28] Kingdom F, Moulden B. Border effects on brightness: a review of findings, models and issues. Spat Vis 1988;3(4):225–62.
[29] Yoshida A, Mantiuk R, Myszkowski K, Seidel HP. Analysis of reproducing real-world appearance on displays of varying dynamic range. Comput Graph Forum 2008;25(3):415–26.
[30] Seetzen H, Li H, Ye L, Ward G, Whitehead L, Heidrich W. Guidelines for contrast, brightness, and amplitude resolution of displays. In: SID digest, 2006. p. 1229–33.
[31] Akyüz AO, Fleming R, Riecke BE, Reinhard E, Bülthoff HH. Do HDR displays support LDR content? A psychophysical evaluation ACM Trans Graph 2007;26(3).
[32] Ledda P, Ward G, Chalmers A. A wide field, high dynamic range, stereographic viewer. In: Proceedings of the 1st international conference on computer graphics and interactive techniques in Australasia and South East Asia. GRAPHITE '03. New York, NY, USA: ACM; 2003. p. 237–44.
[33] Seetzen H, Whitehead LA, Ward G. A high dynamic range display using low and high resolution modulators. In: SID digest, vol. 34. Blackwell Publishing Ltd; 2003. p. 1450–3.
[34] Seetzen H, Heidrich W, Stuerzlinger W, Ward G, Whitehead L, Trentacoste M, et al. High dynamic range display systems. ACM Trans Graph (SIGGRAPH) 2004;23(3):760–8.
[35] Rosink J, Chestakov D, Rajae-Joordens R, Albani L, Arends M, Heeten G. Innovative lcd displays solutions for diagnostic image accuracy. In: Proceedings of the Radiological Society of North America annual meeting, 2006.
[36] Seetzen H. High dynamic range display and projection systems [Ph.D. thesis]. University of British Columbia; 2009.
[37] Reinhard E, Khan EA, Akyüz AO, Johnson GM. Color imaging: fundamentals and applications. A. K. Peters, Ltd.; 2008.
[38] Majumder A, Welch G, Computer graphics optique: optical superposition of projected computer graphics. In: Proceedings of the 7th Eurographics conference on virtual environments & 5th immersive projection technology. EGVE'01, 2001. p. 209–18.
[39] Pavlovych A, Stuerzlinger W. A high-dynamic range projection system. In: Proceedings of the SPIE, vol. 5969, 2005.
[40] Kusakabe Y, Kanazawa M, Nojiri Y, Furuya M, Yoshimura M. A yc-separation-type projector: high dynamic range with double modulation. J Soc Inf Disp 2008;16(2):383–91.
[41] Damberg G, Seetzen H, Ward G, Heidrich W, Whitehead L. High dynamic range projection systems. In: SID digest, vol. 38, 2007. p. 4–7.
[42] Welch G, Fuchs H, Raskar R, Towles H, Brown MS. Projected imagery in your "office of the future". IEEE Comput Graph Appl 2000;20(4):62–7.
[43] Majumder A. Contrast enhancement of multi-displays using human contrast sensitivity. In: Proceedings of the 2005 IEEE computer society conference on computer vision and pattern recognition (CVPR'05), 2005. p. 377–82.
[44] Adams A. The print. Little Brown and Company; 1995.
[45] Mann S, Picard RW. On being 'undigital' with digital cameras: extending dynamic range by combining differently exposed pictures. In: Proceedings of IS&T, 1995. p. 442–8.
[46] Debevec PE, Malik J. Recovering high dynamic range radiance maps from photographs. In: Proceedings of the 24th annual conference on computer graphics and interactive techniques. SIGGRAPH '97; 1997. p. 369–78.
[47] Wetzstein G, Ihrke I, Lanman D, Heidrich W. Computational plenoptic imaging. Comput Graph Forum 2011;30(8):2397–426.
[48] Sen P, Kalantari NK, Yaesoubi M, Darabi S, Goldman DB, Shechtman E. Robust patch-based HDR reconstruction of dynamic scenes. ACM Trans Graph 2012;31(6):203:1–203:11.
[49] Zimmer H, Bruhn A,Weickert J. Freehand HDR imaging of moving scenes with simultaneous resolution enhancement. In: Computer graphics forum. Proceedings of Eurographics, vol. 30(2), 2011. p. 405–14.
[50] Hu J, Gallo O, Pulli K, Sun X. Hdr deghosting: How to deal with saturation? In: CVPR, 2013.
[51] Hadziabdic KK, Telalovic JH, Mantiuk R. Comparison of deghosting algorithms for multi-exposure high dynamic range imaging. In: Proceedings of Spring conference on computer graphics, 2013.
[52] Rouf M, Mantiuk R, Heidrich W, Trentacoste M, Lau C. Glare encoding of high dynamic range images. In: IEEE conference on computer vision and pattern recognition. IEEE Computer Society; 2011. p. 289–96.
[53] Nayar S, Mitsunaga T. High dynamic range imaging: spatially varying pixel exposures. In: IEEE conference on computer vision and pattern recognition, 2000. Proceedings, vol. 1, 2000. p. 472–9.
[54] Adams A, Talvala EV, Park SH, Jacobs DE, Ajdin B, Gelfand N, et al. The Frankencamera: an experimental platform for computational photography. ACM Trans Graph 2010;29(4) 29:1–12.
[55] Echevarria JI, Gutierrez D. Mobile computational photography: exposure fusion on the Nokia N900. In: Proceedings of SIACG, 2011.
[56] Tocci MD, Kiser C, Tocci N, Sen P. A versatile hdr video production system. ACM Trans Graph 2011;30(4):411–10.
[57] Unger J, Gustavson S. High-dynamic-range video for photometric measurement of illumination. In: SPIE, vol. 6501, 2007.
[58] Kronander J, Gustavson S, Bonnet G, Unger J. Unified HDR reconstruction from raw CFA data. In: IEEE international conference on computational photography (ICCP), 2013.
[59] Ledda P, Chalmers A, Troscianko T, Seetzen H. Evaluation of tone mapping operators using a high dynamic range display. ACM Trans Graph 2005;24 (3):640–8.
[60] Mantiuk R, Seidel HP. Modeling a generic tone-mapping operator. In: Computer graphics forum. Proceedings of Eurographics, vol. 27(3), 2008.
[61] Devlin K, Chalmers A, Wilkie A, Purgathofer W. STAR report on tone reproduction and physically based spectral rendering. In: Eurographics 2002, 2002.
[62] Čad'k M, Hajdok O, Lejsek A, Fialka O, Wimmer M, Artusi A, et al. Evaluation of tone mapping operators. ⟨http://dcgi.felk.cvut.cz/home/cadikm/tmo/⟩; 2013.
[63] Reinhard E, Stark M, Shirley P, Ferwerda J. Photographic tone reproduction for digital images. ACM Trans Graph 2002;21(3):267–76.
[64] Tumblin J, Rushmeier H. Tone reproduction for realistic images. IEEE Comput Graph Appl 1993;13(6):42–8.
[65] Ward G. A contrast-based scale factor for luminance display. In: Graphics gems iv. San Diego, CA, USA: Academic Press Professional, Inc.; 1994. p. 415–21, ISBN 0-12-336155-9.
[66] Schlick C. Quantization techniques for visualization of high dynamic range pictures. In: Sakas G, Müller S, Shirley P, editors. Photorealistic rendering techniques. Focus on computer graphics. Berlin, Heidelberg: Springer; 1994. p. 7–20 ISBN 978-3-642-87827-5.
[67] Ferwerda JA, Pattanaik SN, Shirley P, Greenberg DP. A model of visual adaptation for realistic image synthesis. In: Proceedings of the 23rd annual conference on computer graphics and interactive techniques. SIGGRAPH '96. New York, NY, USA: ACM; 1996. p. 249–58, ISBN 0-89791-746-4.

[68] Ward G, Rushmeier H, Piatko C. A visibility matching tone reproduction operator for high dynamic range scenes. IEEE Trans Vis Comput Graph 1997;3(4):291–306.

[69] Drago F, Myszkowski K, Annen T, Chiba N. Adaptive logarithmic mapping for displaying high contrast scenes. Comput Graph Forum 2003;22(3):419–26.

[70] Reinhard E, Devlin K. Dynamic range reduction inspired by photoreceptor physiology. IEEE Trans Vis Comput Graph 2005;11(1):13–24.

[71] Mantiuk R, Myszkowski K, Seidel HP. A perceptual framework for contrast processing of high dynamic range images. ACM Trans Appl Percept 2006;3(3):286–308.

[72] Chiu K, Herf M, Shirley P, Swamy S, Wang C, Zimmerman K. Spatially nonuniform scaling functions for high contrast images. In: Proceedings of graphics interface '93, 1993. p. 245–53.

[73] Pattanaik SN, Ferwerda JA, Fairchild MD, Greenberg DP. A multiscale model of adaptation and spatial vision for realistic image display. In: Proceedings of the 25th annual conference on computer graphics and interactive techniques. SIGGRAPH '98. New York, NY, USA: ACM; 1998. p. 287–98, ISBN 0-89791-999-8.

[74] Krawczyk G, Myszkowski K, Seidel HP. Lightness perception in tone reproduction for high dynamic range images. Comput Graph Forum 2005;24(3):635–45.

[75] Pattanaik SN, Tumblin J, Yee H, Greenberg DP. Time-dependent visual adaptation for fast realistic image display. In: Proceedings of the 27th annual conference on computer graphics and interactive techniques. SIGGRAPH '00. New York, NY, USA: ACM Press, Addison-Wesley Publishing Co; 2000. p. 47–54, ISBN 1-58113-208-5.

[76] Fattal R, Lischinski D, Werman M. Gradient domain high dynamic range compression. ACM Trans Graph 2002;21(3):249–56.

[77] Durand F, Dorsey J. Fast bilateral filtering for the display of high-dynamic-range images. ACM Trans Graph 2002;21(3):257–66.

[78] Mertens T, Kautz J, Reeth FV. Exposure fusion. In: Proceedings of the 15th Pacific conference on computer graphics and applications. PG '07. Washington, DC, USA: IEEE Computer Society; 2007. p. 382–90, ISBN 0-7695-3009-5.

[79] Mantiuk R, Daly S, Kerofsky L. Display adaptive tone mapping. ACM Trans Graph 2008;27(3).

[80] Martin M, Fleming RW, Sorkine O, Gutierrez D. Understanding exposure for reverse tone mapping. In: Congreso Español de Informatica Grafica. Eurographics, 2008.

[81] Masia B, Agustin S, Fleming RW, Sorkine O, Gutierrez D. Evaluation of reverse tone mapping through varying exposure conditions. In: ACM transactions on graphics. Proceedings of SIGGRAPH Asia, vol. 28(5), 2009.

[82] Banterle F, Ledda P, Debattista K, Bloj M, Artusi A, Chalmers A. A psychophysical evaluation of inverse tone mapping techniques. Comput Graph Forum 2009;28(1):13–25.

[83] Rempel AG, Heidrich W, Li H, Mantiuk R. Video viewing preferences for hdr displays under varying ambient illumination. In: Proceedings of the 6th symposium on applied perception in graphics and visualization. APGV '09. New York, NY, USA: ACM; 2009. p. 45–52, ISBN 978-1-60558-743-1.

[84] Daly SJ, Feng X. Bit-depth extension using spatiotemporal microdither based on models of the equivalent input noise of the visual system. In: Eschbach R, Marcu GG, editors. Society of Photo-Optical Instrumentation Engineers (SPIE) conference series, vol. 5008, 2003. p. 455–66.

[85] Daly SJ, Feng X. Decontouring: prevention and removal of false contour artifacts. In: Rogowitz BE, Pappas TN, editors. Society of Photo-Optical Instrumentation Engineers (SPIE) conference series, vol. 5292, 2004. p. 130–49.

[86] Banterle F, Ledda P, Debattista K, Chalmers A. Inverse tone mapping. In: Proceedings of the 4th international computer graphics and interactive techniques in Australasia and Southeast Asia. GRAPHITE '06, 2006. p. 349–56.

[87] Meylan L, Daly S, Ssstrunk S. The reproduction of specular highlights on high dynamic range displays. In: IS&T/SID 14th color imaging conference (CIC), 2006.

[88] Rempel AG, Trentacoste M, Seetzen H, Young HD, Heidrich W, Whitehead L, et al. Ldr2Hdr: on-the-fly reverse tone mapping of legacy video and photographs. ACM Trans Graph 2007;26(3).

[89] Kovaleski R, Oliveira MM. High-quality brightness enhancement functions for real-time reverse tone mapping. Vis Comput 2009;25:539–47.

[90] Banterle F, Chalmers A, Scopigno R, Real-time high fidelity inverse tone mapping for low dynamic range content. In: Miguel A, Otaduy OS, editors. Eurographisc 2013 short papers. Eurographics, 2013.

[91] Didyk P, Mantiuk R, Hein M, Seidel HP. Enhancement of bright video features for hdr displays. In: Proceedings of the 19th Eurographics conference on rendering. EGSR'08, 2008. p. 1265–74.

[92] Wang L, Wei LY, Zhou K, Guo B, Shum HY. High dynamic range image hallucination. In: Proceedings of the 18th Eurographics conference on rendering techniques. EGSR'07; 2007. p. 321–6, ISBN 978-3-905673-52-4.

[93] Masia B, Fleming RW, Sorkine O, Gutierrez D. Selective reverse tone mapping. In: Congreso Español de Informatica Grafica. Eurographics, 2010.

[94] Banterle F, Ledda P, Debattista K, Chalmers A. Expanding low dynamic range videos for high dynamic range applications. In: Proceedings of the 24th Spring conference on computer graphics. SCCG '08. New York, NY, USA: ACM; 2010. p. 33–41, ISBN 978-1-60558-957-2.

[95] Masia B, Gutierrez D. Multilinear regression for gamma expansion of over-exposed content. Technical Report RR-03-11. Universidad de Zaragoza; 2011.

[96] Smith K, Krawczyk G, Myszkowski K, Seidel HP. Beyond tone mapping: enhanced depiction of tone mapped hdr images. Computer Graphics Forum. Proceedings of Eurographics, vol. 25(3), 2006. p. 427–38.

[97] Luft T, Colditz C, Deussen O. Image enhancement by unsharp masking the depth buffer. ACM Trans Graph 2006;25(3):1206–13.

[98] Ritschel T, Smith K, Ihrke M, Grosch T, Myszkowski K, Seidel HP. 3d unsharp masking for scene coherent enhancement. ACM Trans Graph 2008;27(3).

[99] Krawczyk G, Myszkowski K, Seidel HP. Contrast restoration by adaptive countershading. Comput Graph Forum 2007;26.

[100] Trentacoste M, Mantiuk R, Heidrich W, Dufrot F. Unsharp masking, countershading and halos: enhancements or artifacts?. Comput Graph Forum 2012;31:555–64.

[101] Gutierrez D, Seron FJ, Anson O, Munoz A. Chasing the green flash: a global illumination solution for inhomogeneous media. In: Proceedings of the Spring conference on computer graphics, 2004.

[102] Gutierrez D, Anson O, Munoz A, Seron FJ. Perception-based rendering: eyes wide bleached. In: Eurographics short papers, 2005.

[103] Ritschel T, Eisemann E. A computational model of afterimages. Comput Graph Forum 2012;31:529–34.

[104] Yoshida A, Ihrke M, Mantiuk R, Seidel HP. Brightness of the glare illusion. In: Proceedings of the 5th symposium on applied perception in graphics and visualization. APGV '08. New York, NY, USA: ACM; 2008. p. 83–90.

[105] Ritschel T, Ihrke M, Frisvad JR, Coppens J, Myszkowski K, Seidel HP. Temporal glare: real-time dynamic simulation of the scattering in the human eye. Comput Graph Forum 2009;28(2):183–92.

[106] Yang X, Zhang L, Wong TT, Heng PA. Binocular tone mapping. ACM Trans Graph 2012;31(4):93:1–10.

[107] Comstock F. Auxiliary registering device for simultaneous projection of two or more pictures. Patent US1208490 (A); 1916.

[108] Hurvich LM, Jameson D. An opponent-process theory of color vision. Psychol Rev 1957;64(1(6)):384–404.

[109] Luo MR, Clarke AA, Rhodes PA, Schappo A, Scrivener SAR, Tait CJ. Quantifying colour appearance. Part i. Lutchi colour appearance data. Color Res Appl 1991;16(3):166–80.

[110] Hunt R. The reproduction of colour. The Wiley-IS&T series in imaging science and technology. 6th ed.Wiley; 2004.

[111] Fairchild MD. Color appearance models. The Wiley-IS&T series in imaging science and technology. 2nd ed.Wiley; 2005.

[112] Monnier P, Shevell SK. Large shifts in color appearance from patterned chromatic backgrounds. Nat Neurosci 2003;6(8):801–2.

[113] Mullen KT. The contrast sensitivity of human colour vision to red–green and blue–yellow chromatic gratings. J Physiol 1985;359(1):381–400.

[114] Kim MH, Ritschel T, Kautz J. Edge-aware color appearance. In: ACM transactions on graphics. Presented at SIGGRAPH2011, vol. 30 (2), 2011. p. 13:1–9.

[115] Brenner E, Ruiz JS, Herraiz EM, Cornelissen FW, Smeets JB. Chromatic induction an the layout of colours within a complex scene. Vis Res 2003;43:1413–21.

[116] ISO 11664-1:2007(E)/CIE S 014-1/E:2006. Joint ISO/CIE Standard: Colorimetry Part 1: CIE Standard Colorimetric Observers, 2007.

[117] Sony Inc. Extended-gamut color space for video applications ⟨http://www.sony.net/SonyInfo/technology/technology/theme/xvycc_01.html⟩. Last accessed July 2013.

[118] Kim JH, Allebach JP. Color filters for CRT-based rear projection television. IEEE Trans Consum Electron 1996;42(4):1050–4.

[119] Shieh KK, Lin CC. Effects of screen type, ambient illumination, and color combination on VDT visual performance and subjective preference. Int J Ind Ergon 2000;26:527–36.

[120] Menozzi M, Lang F, Näpflin U, Zeller C, Krueger H. CRT versus LCD: effects of refresh, rate display technology and background luminance in visual performance. Displays 2001;22:79–85.

[121] Smith-Gillespie R. Design considerations for LED backlights in large format color LCDs. In: LEDs in displays SID technical symposium, 2006. p. 1–10.

[122] Kakinuma K. Technology of wide color gamut backlight with light-emitting diode for liquid crystal display television. Jpn J Appl Phys 2006;45:4330–4.

[123] Sugiura H, Kaneko H, Kagawa S, Ozawa M, Tanizoe H, Katou H, et al. Wide color gamut and high brightness assured by the support of LED backlighting in WUXGA LCD monitor. In: SID digest, 2004. p. 1230–3.

[124] Sugiura H, Kaneko H, Kagawa S, Ozawa M, Tanizoe H, Ueno H, et al. Wide-color-gamut and high-brightness wuxga lcd monitor with color calibrator, Proc. SPIE 5667, Color Imaging X: Processing, Hardcopy, and Applications, 2005. p. 554, http://dx.doi.org/10.1117/12.585706.

[125] Sugiura H, Kagawa S, Kaneko H, Ozawa M, Tanizoe H, Kimura T, et al. Wide color gamut displays using led backlight—signal processing circuits, color calibration system and multi-primaries. In: IEEE international conference on image processing, 2005. ICIP 2005, vol. 2, 2005. p. 9–12.

[126] Seetzen H, Makki S, Ip H, Wan T, Kwong V, Ward G, et al. Self-calibrating wide color gamut high dynamic range display. In: Human vision and electronic imaging XII: Proceedings of SPIE-IS&T electronic imaging. SPIE; 2007. p. 64920Z-1–9.

[127] Masaoka K, Nishida Y, Sugawara M, Nakasu E. Design of primaries for a wide-gamut television colorimetry. IEEE Trans Broadcast 2010;56(4):452–7.

[128] Someya J, Inoue Y, Yoshii H, Kuwata M, Kagawa S, Sasagawa T, et al. Laser TV: ultra-wide gamut for a new extended color-space standard, xvYCC. In: SID digest, 2006. p. 1134–7.

[129] Sugiura H, Kuwata M, Inoue Y, Sasagawa T, Nagase A, Kagawa S, et al. Laser TV ultra wide color gamut in conformity with xvYCC. In: SID digest, 2007. p. 12–5.

[130] Sugiura H, Sasagawa T, Michimori A, Toide E, Yanagisawa T, Yamamoto S, et al. 65-inch, super slim, laser TV with newly developed laser light source. In: SID digest, 2008. p. 854–7.
[131] Kojima K, Miyata A. Laser TV. Technical Report. Mitsubishi Electric ADVANCE; 2009.
[132] Chino E, Tajiri K, Kawakami H, Ohira H, Kamijo K, Kaneko H, et al. Development of wide-color-gamut mobile displays with four-primary-color lcds. In: SID symposium digest of technical papers, vol. 37(1), 2006. p. 1221–4.
[133] Ueki S, Nakamura K, Yoshida Y, Mori T, Tomizawa K, Narutaki Y, et al. Five-primary-color 60-inch LCD with novel wide color gamut and wide viewing angle. In: SID digest, 2009. p. 927–30.
[134] Cheng HC, Ben-David I, Wu ST. Five-primary-color lcds. J Disp Technol 2010;6(1):3–7.
[135] Yang YC, Song K, Rho S, Rho NS, Hong S, Deul KB, et al. Development of six primary-color LCD. In: SID digest, 2005. p. 1210–3.
[136] Sugiura H, Kaneko H, Kagawa S, Ozawa M, Someya J, Tanizoe H, et al. Improved six-primary-color 23-in. WXGA LCD using six-color LEDs. In: SID digest, 2005. p. 1126–9.
[137] Sugiura H, Kaneko H, Kagawa S, Someya J, Tanizoe H. Six-primary-color lcd monitor using six-color leds with an accurate calibration system, Proc. SPIE 6058, Color Imaging XI: Processing, Hardcopy, and Applications, vol. 6058, 2006. p. 60580H, http://dx.doi.org/10.1117/12.642712.
[138] Ajito T, Obi T, Yamaguchi M, Ohyama N. Expanded color gamut reproduced by six-primary projection display, Proc. SPIE 3954, Projection Displays 2000: Sixth in a Series, 2000; 130, http://dx.doi.org/10.1117/12.383364.
[139] Roth S, Ben-David I, Ben-Chorin M, Eliav D, Ben-David O. Wide gamut, high brightness multiple primaries single panel projection displays. In: SID digest, 2003. p. 118–21.
[140] Brennesholtz MS, McClain SC, Roth S, Malka D. A single panel LCOS engine with a rotating drum and a wide color gamut. In: SID digest, vol. 36, 2005. p. 1814–7.
[141] Roth S, Caldwell W. Four primary color projection display. In: SID digest, 2005. p. 1818–21.
[142] Kim MH, Weyrich T, Kautz J. Modeling human color perception under extended luminance levels. ACM Trans Graph 2009;28(3) 27:1–9.
[143] Akyüz AO, Reinhard E. Color appearance in high dynamic range imaging. SPIE J Electron Imaging 2006;15(3) 033001-1–12.
[144] Moroney N, Fairchild MD, Hunt RWG, Li C, Luo MR, Newman T. The ciecam02 color appearance model. In: IS&T/SID 10th color imaging conference, 2002. p. 23–7.
[145] Kunkel T, Reinhard E. A neurophysiology-inspired steady-state color appearance model. J Opt Soc Am A 2009;26:776–82.
[146] Reinhard E. Tone reproduction and color appearance modeling: two sides of the same coin? In: 19th color and imaging conference, 2011. p. 7–11.
[147] Mantiuk R, Mantiuk R, Tomaszewska A, Heidrich W. Color correction for tone mapping. In: Computer graphics forum. Proceedings of EUROGRAPHICS, vol. 28(2), 2009. p. 193–202.
[148] Fairchild M, Johnson G. Meet iCAM: an image color appearance model. In: IS&T/SID 10th color imaging conference, 2002. p. 33–8.
[149] Fairchild MD, Johnson GM. The icam framework for image appearance, image differences, and image quality. J Electron Imaging 2004;13:126–38.
[150] Kuang J, Johnson GM, Fairchild MD. icam06: a refined image appearance model for {HDR} image rendering. J Vis Commun Image Represent 2007;18(5):406–14.
[151] Reinhard E, Pouli T, Kunkel T, Long B, Ballestad A, Damberg G. Calibrated image appearance reproduction. ACM Trans Graph 2012;31(6) 201:1–11.
[152] IEC 61996-2-2. Multimedia systems and equipment—color measurement and management—Part 2-2: Color management—extended RGB color space-scRGB, 2003.
[153] IEC 61966-2-4 First edition. Multimedia systems and equipment—Color measurement and management: Part 2–4: Color management—Extended-gamut YCC colour space for video applications-xvYCC, 2006.
[154] Morovic J, Luo MR. The fundamentals of gamut mapping: a survey. J Imaging Sci Technol 2001;45(3):283–90.
[155] Giesen J, Schuberth E, Simon K, Zolliker P, Zweifel O. Image-dependent gamut mapping as optimization problem. IEEE Trans Image Process 2007;16(10):2401–10.
[156] Casella SE, Heckaman RL, Fairchild MD. Mapping standard image content to wide-gamut displays. In: Sixteenth color imaging conference: color science and engineering systems, technologies, and applications, 2008. p. 106–11.
[157] Heckaman RL, Sullivan J. Rendering digital cinema and broadcast tv content to wide gamut display media, SID Symposium Digest of Technical Papers, 2011;42(1):225–8, http://dx.doi.org/10.1889/1.3621279.
[158] Anderson H, Garcia E, Gupta M. Gamut expansion for video and image sets. In: Proceedings of the 14th international conference of image analysis and processing workshops. ICIAPW '07. Washington, DC, USA: IEEE Computer Society; 2007. p. 188–91.
[159] Muijs R, Laird J, Kuang J, Swinkels S. Subjective evaluation of gamut extension methods for wide-gamut displays. In: IDW, 2006.
[160] Laird J, Muijs R, Kuang J. Development and evaluation of gamut extension algorithms. Color Res Appl 2009;34(6):443–51.
[161] Morovič J. Color gamut mapping. Wiley; 2008.
[162] Glassner AS, Fishkin KP, Marimont DH, Stone MC. Device-directed rendering. ACM Trans Graph 1995;14(1):58–76.
[163] Gentile RS, Allebach JP, Walowit E. A comparison of techniques for color gamut mismatch compensation. In: Proceedings of the SPIE, vol. 1077, 1989. p. 342–54.
[164] Montag E, Fairchild M. Gamut mapping: evaluation of chroma clipping techniques for three destination gamuts. In: IS&T/SID sixth color imaging conference: color science, systems and applications, 1998. p. 57–61.
[165] Nayar SK, Peri H, Grossberg MD, Belhumeur PN. A projection system with radiometric compensation for screen imperfections. In: First IEEE international workshop on projector-camera systems (PROCAMS-2003), 2003.
[166] Grossberg M, Peri H, Nayar S, Belhumeur P. Making one object look like another: controlling appearance using a projector–camera system. In: Proceedings of the 2004 IEEE computer society conference on computer vision and pattern recognition, 2004. CVPR 2004, vol. 1, 2004. p. 452–9.
[167] Wang D, Sato I, Okabe T, Sato Y. Radiometric compensation in a projector–camera system based on the properties of human vision system. In: IEEE international workshop on projector–camera systems (PROCAMS). Washington, DC, USA: IEEE Computer Society; 2005.
[168] Ashdown M, Okabe T, Sato I, Sato Y. Robust content-dependent photometric projector compensation. In: IEEE international workshop on projector–camera systems (PROCAMS), 2006.
[169] Wetzstein G, Bimber O. Radiometric compensation through inverse light transport. In: Proceedings of Pacific conference on computer graphics and applications, 2007. p. 391–9.
[170] Zollmann S, Bimber O. Imperceptible calibration for radiometric compensation. In: Proceedings of Eurographics (Short Paper), 2007.
[171] Yang R, Welch G. Automatic and continuous projector display surface calibration using every-day imagery. In: WSCG 2001 conference proceedings, 2001.
[172] Curcio CA, Sloan KR, Kalina RE, Hendrickson AE. Human photoreceptor topography. J Comp Neurol 1990;292(4):497–523.
[173] Didyk P, Eiseman E, Ritschel T, Myszkowski K, Seidel HH. Apparent resolution display enhancement for moving images. ACM Trans Graph (SIGGRAPH) 2010;29(3).
[174] Westheimer G. Hiperacuity. Encyclopedia of neuroscience. Academic Press, Oxford; 2008.
[175] Poletti M, Rucci M. Eye movements under various conditions of image fading. J Vis 2010;10(3).
[176] Kalloniatis M, Luu C. Temporal resolution ⟨http://webvision.med.utah.edu/temporal.html⟩; 2009.
[177] Krauzlis R, Lisberger SG. Temporal properties of visual motion signals for the initiation of smooth pursuit eye movements in monkeys. J Neurophysiol 1994;72(1):150–62.
[178] Martinez-Conde S, Macknik SL, Hubel DH. The role of fixational eye movements in visual perception. Nat Rev Neurosci 2004;5(3):229–40.
[179] Laird J, Rosen M, Pelz J, Montag E, Daly S. Spatio-velocity CSF as a function of retinal velocity using unstabilized stimuli. In: Human vision and electronic imaging XI. SPIE proceedings series, vol. 6057, 2006. p. 32–43.
[180] Daly S. Engineering observations from spatiovelocity and spatiotemporal visual models. In: Human vision and electronic imaging III. SPIE Proceedings series, vol. 3299, 1998. p. 180–91.
[181] Berthouzoz F, Fattal R. Resolution enhancement by vibrating displays. ACM Trans Graph 2012;31(2) 15:1–14.
[182] Humphreys G, Hanrahan P. A distributed graphics system for large tiled displays. In: Proceedings of the conference on visualization '99: celebrating ten years. VIS '99. Los Alamitos, CA, USA: IEEE Computer Society Press; 1999. p. 215–23.
[183] Raskar R, Brown MS, Yang R, Chen WC, Welch G, Towles H, et al. Multi-projector displays using camera-based registration. In: Proceedings of the conference on visualization '99: celebrating ten years. VIS '99. Los Alamitos, CA, USA: IEEE Computer Society Press; 1999. p. 161–8.
[184] Majumder A, Stevens R. Perceptual photometric seamlessness in projection-based tiled displays. ACM Trans Graph 2005;24(1):118–39.
[185] Brown M, Majumder A, Yang R. Camera-based calibration techniques for seamless multiprojector displays. IEEE Trans Vis Comput Graph 2005;11(2):193–206.
[186] Majumder A, He Z, Towles H, Welch G. Achieving color uniformity across multi-projector displays. In: Proceedings of the conference on visualization '00. VIS '00. Los Alamitos, CA, USA: IEEE Computer Society Press; 2000. p. 117–24.
[187] Platt JC. Optimal filtering for patterned displays. IEEE Signal Process Lett 2000;7(7):179–81.
[188] Damera-Venkata N, Chang N. Display supersampling. ACM Trans Graph 2009;28(1) 9:1–19.
[189] Jaynes C, Ramakrishnan D. Super-resolution composition in multi-projector displays. In: IEEE PROCAMS, 2003.
[190] Ulichney R, Ghajarnia A, Damera-Venkata N. Quantifying the performance of overlapped displays. In: IS&T/SPIE electronic imaging, 2010. p. 7529–27.
[191] Sajadi B, Gopi M, Majumder A. Edge-guided resolution enhancement in projectors via optical pixel sharing. ACM Trans Graph (SIGGRAPH) 2012;31(4) 79:1–122.
[192] Ben-Ezra M, Zomet A, Nayar S. Jitter camera: high resolution video from a low resolution detector. In: Proceedings of the 2004 IEEE computer society conference on computer vision and pattern recognition, 2004. CVPR 2004, vol. 2, 2004. p. 135–42.
[193] Allen W, Ulichney R. Wobulation: doubling the addressed resolution of projection displays. In: Proceedings of the SID, vol. 47, 2005.

[194] Agranat AJ, Gumennik A, Ilan H. Refractive index engineering by fast ion implantations: a generic method for constructing multi-components electro-optical circuits. Proc. SPIE 7604, Integrated Optics: Devices, Materials, and Technologies XIV, 2010;76040Y:1–17, http://dx.doi.org/10.1117/12.841287.
[195] Sajadi B, Majumder A. Meenakshisundaram G, Lai D, Thler A. Image enhancement in projectors via optical pixel shift and overlay. In: Proceedings of the ICCP, 2013.
[196] Irani M, Peleg S. Super resolution from image sequences. In: ICPR-C, 1990. p. 115–20.
[197] Baker S, Kanade T. Limits on super-resolution and how to break them. IEEE Trans Pattern Anal Mach Intell 2002;24(9):1167–83.
[198] Park SC, Park MK, Kang MG. Super-resolution image reconstruction: a technical overview. IEEE Signal Process Mag 2003;20(3):21–36.
[199] van Ouwerkerk J. Image super-resolution survey. Image Vis Comput 2006;24 (10):1039–52.
[200] Majumder A. Is spatial super-resolution feasible using overlapping projectors? In: IEEE international conference on acoustics, speech, and signal processing, 2005. Proceedings. (ICASSP '05), vol. 4, 2005. p. 209–12.
[201] Damera-Venkata N, Chang N, Dicarlo J. A unified paradigm for scalable multi-projector displays. IEEE Trans Vis Comput Graph 2007;13(6):1360–7.
[202] Benzschawel JL, Howard WE. Method of and apparatus for displaying a multicolor image. U.S. Patent 5341153; 1994.
[203] Elliott CHB, Han S, Im MH, Higgins M, Higgins P, Hong M, et al. Co-optimization of color amlcd subpixel architecture and rendering algorithms. In: SID digest, vol. 33, 2002. p. 172–5.
[204] Arnold AD, Castro PE, Hatwar TK, Hettel MV, Kane PJ, Ludwicki JE, et al. Full-color amoled with rgbw pixel pattern. J Soc Inf Disp 2005;13(6):525–35.
[205] Elliott CHB, Credelle TL, Higgins MF. Adding a white subpixel. Inf Disp 2005;21(5):26–31.
[206] Hara Zi, Shiramatsu N. Improvement in the picture quality of moving pictures for matrix displays. J Soc Inf Disp 2000;8(2):129–37.
[207] Klompenhouwer MA, DeHaan G. Subpixel image scaling for color-matrix displays. J Soc Inf Disp 2003;11(1):99–108.
[208] Farrell J, Eldar S, Larson K, Matskewich T, Wandell B. Optimizing subpixel rendering using a perceptual metric. J Soc Inf Disp 2011;19(8):513–9.
[209] Messing D, Daly S. Improved display resolution of subsampled colour images using subpixel addressing. In: 2002 international conference on image processing. 2002. Proceedings, vol. 1, 2002. p. 625–8.
[210] Messing DS, Kerofsky LJ. Using optimal rendering to visually mask defective subpixels. In: SPIE conference series, vol. 6057, 2006. p. 236–47.
[211] Engelhardt T, Schmidt TW, Kautz J, Dachsbacher C. Low-cost subpixel rendering for diverse displays. Computer Graphics Forum 2013, to appear.
[212] Didyk P, Eisemann E, Ritschel T, Myszkowski K, Seidel HP. Apparent display resolution enhancement for moving images. In: ACM transactions on graphics. Proceedings SIGGRAPH 2010, Los Angeles, vol. 29(4), 2010. p. 113:1–8.
[213] Said A. Analysis of subframe generation for superimposed images. In: 2006 IEEE international conference on image processing, 2006. p. 401–4.
[214] Basu S, Baudisch P. System and process for increasing the apparent resolution of a display. US Patent 7548662; 2009.
[215] Templin K, Didyk P, Ritschel T, Eisemann E, Myszkowski K, Seidel HP. Apparent resolution enhancement for animations. In: 27th Spring conference on computer graphics, Vinicne, Slovak Republic, 2011. p. 85–92.
[216] van Hateren JH. A cellular and molecular model of response kinetics and adaptation in primate cones and horizontal cells. J Vis 2005;5(4):331–47.
[217] Gorea A, Tyler CW. New look at Bloch's law for contrast. J Opt Soc Am A 1986;3(1):52–61.
[218] de Lange H. Research into the dynamic nature of the human fovea—cortex systems with intermittent and modulated light. I. Attenuation characteristics with white and colored light. J Opt Soc Am 1958;48(11):777–83.
[219] McKee SP, Taylor DG. Discrimination of time: comparison of foveal and peripheral sensitivity. J Opt Soc Am A 1984;1(6):620–8.
[220] Mäkelä P, Rovamo J, Whitaker D. Effects of luminance and external temporal noise on flicker sensitivity as a function of stimulus size at various eccentricities. Vis Res 1994;34(15):1981–91.
[221] Aydın TO, Čadík M, Myszkowski K, Seidel HP. Video quality assessment for computer graphics applications. In: ACM transactions on graphics. Proceedings of SIGGRAPH Asia, vol. 29, 2010. p. 161:1–12.
[222] Didyk P, Eisemann E, Ritschel T, Myszkowski K, Seidel HP. Perceptually-motivated real-time temporal upsampling of 3D content for high-refresh-rate displays. In: Computer graphics forum. Proceedings of Eurographics, vol. 29(2), 2010. p. 713–22.
[223] Pan H, Feng XF, Daly S. LCD motion blur modeling and analysis. In: Proceedings of ICIP, 2005. p. 21–4.
[224] Klompenhouwer MA, Velthoven LJ. Motion blur reduction for liquid crystal displays: motion-compensated inverse filtering. In: Proceedings of SPIE, vol. 5308, 2004.
[225] Feng XF. LCD motion blur analysis, perception, and reduction using synchronized backlight flashing. In: Human vision and electronic imaging XI, vol. 6057. SPIE; 2006. p. M1–14.
[226] Chen H, Kim SS, Lee SH, Kwon OJ, Sung JH. Nonlinearity compensated smooth frame insertion for motion-blur reduction in LCDs. In: 2005 IEEE 7th workshop on proceedings of multimedia signal processing, 2005. p. 1–4.
[227] Kurita T. Moving picture quality improvement for hold-type AM-LCDs. In: Society for information display (SID) '01, 2001. p. 986–9.
[228] He H, Velthoven L, Bellers E, Janssen J. Analysis and implementation of motion compensated inverse filtering for reducing motion blur on lcd panels. In: International conference on consumer electronics, 2007. ICCE 2007. Digest of technical papers, 2007. p. 1–2.
[229] Smythe D. A two-pass mesh warping algorithm for object transformation and image interpolation. Rapport technique 1030, 1990.
[230] Wolberg G. Image morphing: a survey. Vis Comput 1998;14(8):360–72.
[231] Liu F, Gleicher M, Jin H, Agarwala A. Content-preserving warps for 3D video stabilization. In: ACM transactions on graphics. Proceedings of SIGGRAPH, vol. 28, 2009.
[232] Mahajan D, Huang FC, Matusik W, Ramamoorthi R, Belhumeur P. Moving gradients: a path-based method for plausible image interpolation. In: ACM transactions on graphics. Proceedings of SIGGRAPH, vol. 28(3), 2009. p. 42:1–11.
[233] Stich T, Linz C, Wallraven C, Cunningham D, Magnor M. Perception-motivated interpolation of image sequences. ACM Trans Appl Percept 2011;8(2) 11:1–25.
[234] Mark WR, McMillan L, Bishop G. Post-rendering 3D warping. In: Proceedings of ACM I3D, 1997. p. 7–16.
[235] Walter B, Drettakis G, Parker S. Interactive rendering using render cache. In: Proceedings of EGSR, 1999. p. 19–30.
[236] Nehab DF, Sander PV, Lawrence J, Tatarchuk N, Isidoro J. Accelerating real-time shading with reverse reprojection caching. In: Graphics hardware, 2007. p. 25–35.
[237] Sitthi-amorn P, Lawrence J, Yang L, Sander PV, Nehab D, Xi J. Automated reprojection-based pixel shader optimization. ACM Trans Graph 2008;27(5).
[238] Yang L, Tse YC, Sander PV, Lawrence J, Nehab D, Hoppe H, et al. Image-based bidirectional scene reprojection. ACM Trans Graph 2011;30(6).
[239] Bowles H, Mitchell K, Sumner R, Moore J, Gross M. Iterative image warping. In: Computer graphics forum, vol. 31. The Eurographics Association and Blackwell Publishing Ltd.; 2012. p. 237–46.
[240] Herzog R, Eisemann E, Myszkowski K, Seidel HP. Spatio-temporal upsampling on the GPU. In: Proceedings of ACM SIGGRAPH symposium on interactive 3D graphics and games, 2010. p. 91–8.
[241] Scherzer D, Yang L, Mattausch O, Nehab D, Sander PV, Wimmer M, et al. A survey on temporal coherence methods in real-time rendering. In: Eurographics 2011 state of the art reports, 2011. p. 101–26.
[242] Didyk P, Ritschel T, Eisemann E, Myszkowski K, Seidel HP. Adaptive image-space stereo view synthesis. In: Vision, modeling and visualization workshop, Siegen, Germany, 2010. p. 299–306.
[243] Palmer SE. Vision science: photons to phenomenology. MIT Press; 1999.
[244] Cutting JE, Vishton PM. Perceiving Layout and Knowing Distances: The integration, relative potency, and contextual use of different information about depth. In: Perception of space and motion. Academic Press; 1995.
[245] Julesz B. Foundations of cyclopean perception. MIT Press; 2006.
[246] Howard IP, Rogers BJ. Seeing in depth, vol. 2: Depth perception. I, Porteous, Toronto, 2002.
[247] Hoffman D, Girshick A, Akeley K, Banks M. Vergence–accommodation conflicts hinder visual performance and cause visual fatigue. J Vis 2008;8 (3):1–30.
[248] Shibata T, Kim J, Hoffman D, Banks M. The zone of comfort: predicting visual discomfort with stereo displays. J Vis 2011;11(8).
[249] Du SP, Masia B, Hu SM, Gutierrez D. A metric of visual comfort for stereoscopic motion. In: ACM transactions on graphics. SIGGRAPH Asia, vol. 32(6), 2013.
[250] Tyler C. Stereoscopic vision: cortical limitations and a disparity scaling effect. Science 1973;181(4096):276–8.
[251] Didyk P, Ritschel T, Eisemann E, Seidel HP, Myszkowski K, Matusik W. A luminance-contrast-aware disparity model and applications. In: ACM transactions on graphics. Proceedings SIGGRAPH Asia 2012, Singapore, vol. 31(5), 2012.
[252] Brookes A, Stevens K. The analogy between stereo depth and brightness. Perception 1989;18(5):601–14.
[253] Lunn P, Morgan M. The analogy between stereo depth and brightness: a reexamination. Perception 1995;24(8):901–4.
[254] Bradshaw MF, Rogers BJ. Sensitivity to horizontal and vertical corrugations defined by binocular disparity. Vis Res 1999;39(18):3049–56.
[255] Anstis S, Howard I, Rogers B. A Craik–O'Brien–Cornsweet illusion for visual depth. Vis Res 1978;18(2):213–7.
[256] Rogers B, Graham M. Anisotropies in the perception of three-dimensional surfaces. Science 1983;221(4618):1409–11.
[257] Didyk P, Ritschel T, Eisemann E, Myszkowski K, Seidel HP. A perceptual model for disparity. In: ACM transactions on graphics. Proceedings of SIGGRAPH 2011, Vancouver, vol. 30(4), 2011. p. 96:1–10.
[258] Wheatstone C. Contributions to the physiology of vision. Part the first. On some remarkable, and hitherto unobserved, phenomena of binocular vision. Philos Trans R Soc Lond 1838;128:371–94.
[259] Wheatstone C. Contributions to the physiology of vision. Part the Second, On some remarkable, and hitherto unobserved, phenomena of binocular vision continued. Philos Trans R Soc Lond 1852;142:1–17.
[260] Urey H, Chellappan KV, Erden E, Surman P. State of the art in stereoscopic and autostereoscopic displays. Proc IEEE 2011;99(4):540–55.
[261] Scher S, Liu J, Vaish R, Gunawardane P, Davis J. 3D+2DTV: 3D displays with no ghosting for viewers without glasses. ACM Trans Graph 2013;32(3) 21:1–10.
[262] Jones G, Lee D, Holliman N, Ezra D. Controlling perceived depth in stereoscopic images. In: Proceedings of SPIE, vol. 4297, 2001. p. 42–53.

[263] Oskam T, Hornung A, Bowles H, Mitchell K, Gross MH. OSCAM—optimized stereoscopic camera control for interactive 3D. In: ACM transactions on graphics. Proceedings of SIGGRAPH Asia, vol. 30, 2011. p. 189:1–8.
[264] Heinzle S, Greisen P, Gallup D, Chen C, Saner D, Smolic A, et al. Computational stereo camera system with programmable control loop. ACM Trans Graph 2011;30 94:1–10.
[265] Held R, Banks M. Misperceptions in stereoscopic displays: a vision science perspective. In: Proceedings of the 5th symposium on applied perception in graphics and visualization. ACM; 2008. p. 23–32.
[266] Lang M, Hornung A, Wang O, Poulakos S, Smolic A, Gross M. Nonlinear disparity mapping for stereoscopic 3D. In: ACM transactions on graphics. Proceedings of SIGGRAPH, vol. 29(4), 2010. p. 751–60.
[267] Zwicker M, Matusik W, Durand F, Pfister H, Forlines C. Antialiasing for automultiscopic 3D displays. In: Proceedings of EGSR, 2006. p. 73–82.
[268] Siegel M, Nagata S. Just enough reality: comfortable 3-d viewing via microstereopsis. IEEE Trans Circuits Syst Video Technol 2000;10(3):387–96.
[269] Didyk P, Ritschel T, Eisemann E, Myszkowski K, Seidel HP. Apparent stereo: the Cornsweet illusion can enhance perceived depth. In: Human vision and electronic imaging XVII, IS&T/SPIE's symposium on electronic imaging, Burlingame, CA, 2012. p. 1–12.
[270] Kellnhofer P, Ritschel T, Myszkowski K, Seidel HP. Optimizing disparity for motion in depth. In: Computer graphics forum. Proceedings of EGSR 2012, vol. 32(4), 2013.
[271] Templin K, Didyk P, Ritschel T, Eisemann E, Myszkowski K, Seidel HP. Highlight microdisparity for improved gloss depiction. In: ACM transactions on graphics. Proceedings of SIGGRAPH 2012, Los Angeles, CA, vol. 31(4), 2012. p. 1–5.
[272] Slinger C, Cameron C, Stanley M. Computer-generated holography as a generic display technology. Computer 2005;38(8):46–53.
[273] Klug M, Holzbach M, Ferdman A. Method and apparatus for recording one-step, full-color, full-parallax, holographic stereograms. U.S. Patent 6,330,088; 2001.
[274] Rogers B, Graham M. Similarities between motion parallax and stereopsis in human depth perception. Vis Res 1982;22:261–70.
[275] Hogervorst MA, Bradshaw MF, Eagle RA. Spatial frequency tuning for 3-D corrugations from motion parallax. Vis Res 2000;40:2149–58.
[276] Bradshaw MF, Hibbard PB, Parton AD, Rose D, Langley K. Surface orientation, modulation frequency and the detection and perception of depth defined by binocular disparity and motion parallax. Vis Res 2006;46:2636–44.
[277] Bradshaw MF, Rogers BJ. The interaction of binocular disparity and motion parallax in the computation of depth. Vis Res 1996;36(21):3457–68.
[278] Reichelt S, Häussler R, Fütterer G, Leister N, Depth cues in human visual perception and their realization in 3d displays. In: Proceedings of the SPIE, vol. 7690, 2010. p. 76900B–76900B-12.
[279] Wetzstein G, Lanman D, Heidrich W, Raskar R. Layered 3D: Tomographic image synthesis for attenuation-based light field and high dynamic range displays. ACM Trans Graph (SIGGRAPH) 2011;30(4):1–12.
[280] Jones A, McDowall I, Yamada H, Bolas M, Debevec P. Rendering for an interactive 360° light field display. ACM Trans Graph (SIGGRAPH) 2007;26 40:1–10.
[281] Barnum PC, Narasimhan SG, Kanade T. A multi-layered display with water drops. ACM Trans Graph 2010;29:1–7.
[282] Blundell B, Schwartz A. Volumetric three-dimensional display systems. Wiley-IEEE Press; 1999.
[283] Favalora GE. Volumetric 3D displays and application infrastructure. IEEE Comput 2005;38:37–44.
[284] Cossairt OS, Napoli J, Hill SL, Dorval RK, Favalora GE. Occlusion-capable multiview volumetric three-dimensional display. Appl Opt 2007;46 (8):1244–50.
[285] Yendo T, Kawakami N, Tachi S. Seelinder: the cylindrical lightfield display. In: ACM SIGGRAPH emerging technologies, 2005.
[286] Maeda H, Hirose K, Yamashita J, Hirota K, Hirose M. All-around display for video avatar in real world. In: IEEE/ACM ISMAR, 2003. p. 288–9.
[287] Sullivan A. A solid-state multi-planar volumetric display. In: SID digest, vol. 32, 2003. p. 207–11.
[288] Agocs, et al. A large scale interactive holographic display. In: IEEE virtual reality, 2006. p. 311–2.
[289] Akeley K, Watt SJ, Girshick AR, Banks MS. A stereo display prototype with multiple focal distances. ACM Trans Graph (SIGGRAPH) 2004;23:804–13.
[290] Nayar S, Anand V. 3D display using passive optical scatterers. IEEE Comput Mag 2007;40(7):54–63.
[291] Perlin K, Han JY. Volumetric display with dust as the participating medium. U.S. Patent 6,997,558; 2006.
[292] Lippmann G. Épreuves réversibles donnant la sensation du relief. J Phys 1908;7(4):821–5.
[293] Perlin K, Paxia S, Kollin JS. An autostereoscopic display. In: ACM SIGGRAPH, 2000. p. 319–26.
[294] Peterka T, Kooima RL, Sandin DJ, Johnson A, Leigh J, DeFanti TA. Advances in the Dynallax solid-state dynamic parallax barrier autostereoscopic visualization display system. IEEE Trans Vis Comput Graph 2008;14(3):487–99.
[295] Lanman D, Hirsch M, Kim Y, Raskar R. Content-adaptive parallax barriers: optimizing dual-layer 3D displays using low-rank light field factorization. ACM Trans Graph (SIGGRAPH Asia) 2010;29 163:1–10.
[296] Stolle H, Olaya JC, Buschbeck S, Sahm H, Schwerdtner A. Technical solutions for a full-resolution autostereoscopic 2D/3D display technology. In: Proceedings of the SPIE, 2008. p. 1–12.
[297] Wetzstein G, Lanman D, Hirsch M, Raskar R. Tensor displays: compressive light field synthesis using multilayer displays with directional backlighting. ACM Trans Graph (SIGGRAPH) 2012;31:1–11.
[298] Wetzstein G, Lanman D, Heidrich W, Raskar R. Layered 3D: Tomographic image synthesis for attenuation-based light field and high dynamic range displays. ACM Trans Graph (SIGGRAPH) 2011;30:1–11.
[299] Lanman D, Wetzstein G, Hirsch M, Heidrich W, Raskar R. Polarization fields: dynamic light field display using multi-layer LCDs. ACM Trans Graph (SIGGRAPH Asia) 2011;30:1–9.
[300] Takaki Y. High-density directional display for generating natural three-dimensional images. In: Proceedings of IEEE, vol. 94(3), 2006.
[301] Takaki Y, Tanaka K, Nakamura J. Super multi-view display with a lower resolution flat-panel display. Opt Express 2011;19(5):4129–39.
[302] Pamplona V, Oliveira M, Aliaga D, Raskar R. Tailored displays to compensate for visual aberrations. ACM Trans Graph (SIGGRAPH) 2012;31(4):81, http://dx.doi.org/10.1145/2185520.2185577.
[303] Hoffman DM, Banks MS. Stereo display with time-multiplexed focal adjustment. In: SPIE stereoscopic displays and applications XX, vol. 7237, 2009. p. 1–8.
[304] Shibata T, Kawai T, Ohta K, Otsuki M, Miyake N, Yoshihara Y, et al. Stereoscopic 3-D display with optical correction for the reduction of the discrepancy between accommodation and convergence. In: SID, vol. 13(8), 2005. p. 665–71.
[305] Mainmone A, Wetzstein G, Hirsch M, Lanman D, Raskar R, Fuchs H. Focus 3D: compressive accommodation display. ACM Trans Graph 2013:1–12.
[306] Lanman D, Luebke D. Near-eye light field displays. In: ACM SIGGRAPH 2013 emerging technologies. SIGGRAPH '13, 2013. p. 11–11:1.
[307] Isaksen A, McMillan L, Gortler SJ. Dynamically reparameterized light fields. In: Proceedings of the 27th annual conference on computer graphics and interactive techniques. SIGGRAPH '00, 2000. p. 297–306.
[308] Chai JX, Tong X, Chan SC, Shum HY, Plenoptic sampling. In: Proceedings of the 27th annual conference on computer graphics and interactive techniques. SIGGRAPH '00, 2000. p. 307–18.
[309] Ranieri N, Heinzle S, Smithwick Q, Reetz D, Smoot LS, Matusik W, et al. Multi-layered automultiscopic displays. Comput Graph Forum 2012;31 (7pt2):2135–43.
[310] Ranieri N, Heinzle S, Barnum P, Matusik W, Gross M. Light-field approximation using basic display layer primitives. In: SID symposium digest of technical papers, vol. 44(1), 2013. p. 408–11.
[311] Heide F, Wetzstein G, Raskar R, Heidrich W. Adaptive image synthesis for compressive displays. ACM transactions on graphics. Proceedings of SIGGRAPH, vol. 32(4), 2013. p. 1–11.
[312] Singh DSK, Shin J. Real-time handling of existing content sources on a multi-layer display, Proc. SPIE 8648, Stereoscopic Displays and Applications XXIV, 2013. p. 86480I, http://dx.doi.org/10.1117/12.2010659.
[313] Didyk P, Sitthi-Amorn P, Freeman W, Durand F, Matusik W. Joint view expansion and filtering for automultiscopic 3d displays. ACM Trans Graph (SIGGRAPH Asia) 2013;32(6).
[314] Masia B, Wetzstein G, Aliaga C, Raskar R, Gutierrez D. Display adaptive 3D content remapping. Computer Graphics 2013;37(8):983–96, http://dx.doi.org/10.1016/j.cag.2013.06.004 (this issue).
[315] Banterle F, Artusi A, Aydin T, Didyk P, Eisemann E, Gutierrez D, et al. Multidimensional image retargeting. In: ACM SIGGRAPH Asia 2011 courses. ACM; 2011.
[316] Banterle F, Artusi A, Aydin T, Didyk P, Eisemann E, Gutierrez D, et al. Mapping images to target devices: spatial, temporal, stereo, tone, and color. In: Eurographics 2012 tutorials, 2012.
[317] Birklbauer C, Bimber O. Light-field retargeting. Comp Graph Forum 2012;31 (2pt1):295–303.
[318] Kim M, Lee S, Choi C, Um GM, Hur N, Kim J. Depth scaling of multiview images for automultiscopic 3D monitors. In: 3DTV conference: the true vision—capture, transmission and display of 3D video, 2008.
[319] Kim C, Hornung A, Heinzle S, Matusik W, Gross M. Multi-perspective stereoscopy from light fields. ACM Trans Graph 2011;30:190:1–10.
[320] Seitz SM, Kim J. The space of all stereo images. Int J Comput Vision 2002;48:21–38.
[321] Mantiuk R, Kim KJ, Rempel AG, Heidrich W. Hdr-vdp-2: a calibrated visual metric for visibility and quality predictions in all luminance conditions. ACM Trans Graph 2011;30(4):40:1–14.
[322] Masia B, Wetzstein G, Aliaga C, Raskar R, Gutierrez D. Perceptually-optimized content remapping for automultiscopic displays. In: ACM SIGGRAPH 2012 posters. New York, NY, USA: ACM; 2012.
[323] Tompkin J, Muff S, Jakuschevskij S, McCann J, Kautz J, Alexa M, et al. Interactive light field painting. In: ACM SIGGRAPH emerging technologies, 2012.
[324] Hirsch M, Izadi S, Holtzman H, Raskar R. 8d: interacting with a relightable glasses-free 3d display. In: CHI, 2013. p. 2209–12.
[325] Hirsch M, Lanman D, Holtzman H, Raskar R. Bidi screen: a thin, depth-sensing lcd for 3d interaction using light fields. ACM Trans Graph (SIGGRAPH Asia) 2009;28(5):1–9.
[326] Alonso M. Jr. Barreto AB. Pre-compensation for high-order aberrations of the human eye using on-screen image deconvolution. In: IEEE engineering in medicine and biology society, vol. 1, 2003. p. 556–9.
[327] Yellott JI, Yellott JW. Correcting spurious resolution in defocused images. In: Proceedings of SPIE, vol. 6492, 2007.

[328] Archand P, Pite E, Guillemet H, Trocme L. Systems and methods for rendering a display to compensate for a viewer's visual impairment. International Patent Application PCT/US2011/039993; 2011.

[329] Huang FC, Lanman D, Barsky BA, Raskar R. Correcting for optical aberrations using multilayer displays. ACM Trans Graph (SIGGRAPH Asia) 2012;31 (6):185:1–12.

[330] Wetzstein G, Hirsch M. Display blocks: build your own display. ⟨http://displayblocks.org/⟩; 2013.

[331] Hosono H. Running electricity through transparent materials: triggering a revolution in displays!. JST Breakthrough Report 2013, vol. 6; 2013.

[332] Aumayr PR. Stereopsis in the context of high dynamic range stereo displays [Master thesis]. Germany: Johannes Kepler Universität Linz; 2012.

[333] Anderson BL. Stereovision: beyond disparity computations. Trends Cogn Sci 1998;2:214–22.

[334] Wang O, Fuchs M, Fuchs C, Davis J, Seidel HP, Lensch H. A context-aware light source. In: 2010 IEEE international conference on computational photography (ICCP), 2010. p. 1–8.

[335] Aliaga DG, Yeung YH, Law A, Sajadi B, Majumder A. Fast high-resolution appearance editing using superimposed projections. ACM Trans Graph 2012;31(2) 13:1–13.

[336] Cossairt O, Nayar SK, Ramamoorthi R. Light field transfer: global illumination between real and synthetic objects. In: ACM transactions on graphics. Also Proceedings of ACM SIGGRAPH, 2008.

[337] Nayar SK, Belhumeur PN, Boult TE. Lighting sensitive display. ACM Trans Graph 2004:963–79.

[338] Willis KD, Brockmeyer E, Hudson SE, Poupyrev I. Printed optics: 3D printing of embedded optical elements for interactive devices. In: Proceedings of the ACM UIST, 2012.

[339] Tompkin J, Heinzle S, Kautz J, Matusik W. Content-adaptive lenticular prints. ACM Trans Graph 2013;32(4):133:1–10.